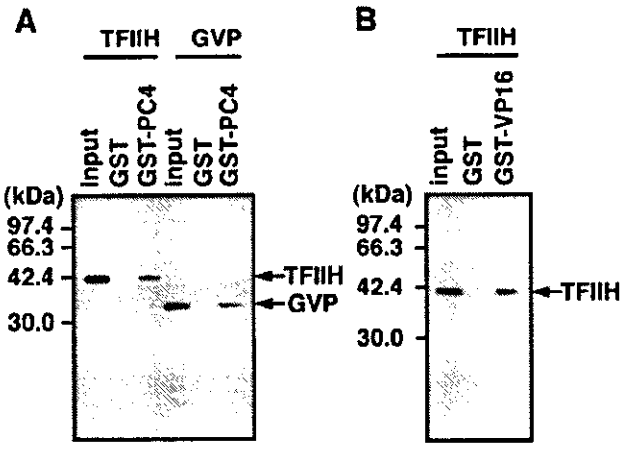

FIG. 3. PC4 interacts directly with TFIIH. (A) Interaction of PC4 with TFIIH. PC4 was fused to the C terminus of GST and expressed in *E. coli* as GST-PC4. TFIIH and GAL4-VP16 were allowed to interact with GST or GST-PC4 prebound to glutathione-Sepharose, and, after extensive washing, bound proteins were eluted, separated by SDS-PAGE along with ~20% of the amount of the input protein, and detected by immunoblotting. TFIIH and GAL4-VP16 were detected with anti-FLAG M2 antibody, since the MO15 subunit of TFIIH and GAL4-VP16 were tagged with a FLAG epitope. The positions of molecular mass markers are indicated on the left. The positions of MO15 (TFIIH) and GAL4-VP16 (GVP) are also indicated on the right. (B) Interaction of TFIIH and GAL4-VP16. GST pull-down assays were done under the same conditions as used for the tests presented in panel A, with GST-VP16 being used in place of GST-PC4.

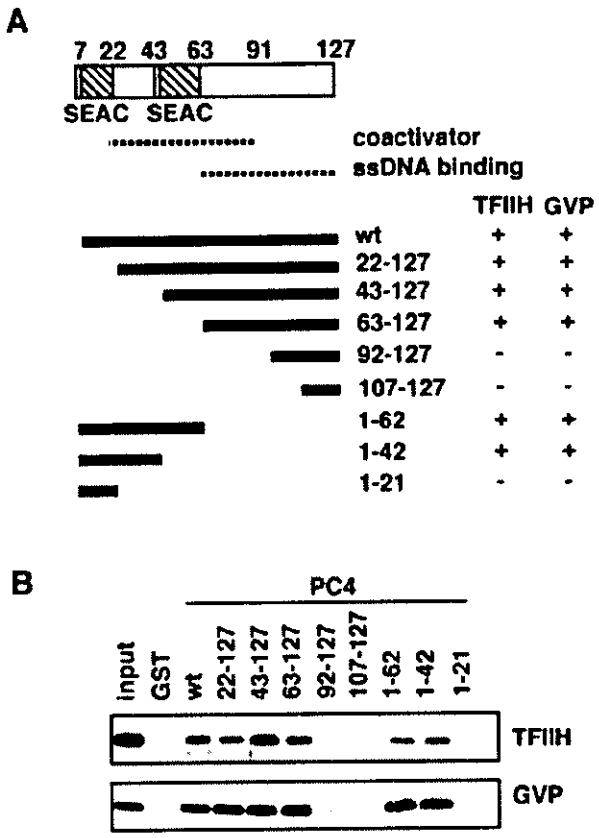

FIG. 4. The interaction of TFIIH and GAL4-VP16 with the coactivator domain of PC4. (A) Schematic representation of the domain structure of PC4. Two serine-rich domains, termed SEAC, are present between amino acid residues 7 and 22 and between residues 43 and 63. The domain for binding single-stranded DNA (dotted line) is localized between residues 63 and 127, and the 89th tryptophan residue is critical for its activity. The coactivator domain (dotted line) is localized to the region between residues 63 and 91, partially overlapping the ssDNA-binding domain. The lower panel shows the tested deletion mutants and the results of the GST pull-down assays for their interactions with PC4 or GAL4-VP16. The 127-amino-acid full-length PC4 is indicated by "wt." Binding and nonbinding are indicated by "+" and "−," respectively, on the right side of the lower panel. (B) GST pull-down assays for PC4 deletion mutants, as detected with Western blots. Note the variation in the amounts of bound TFIIH, which was reproducible, in marked contrast to the constant level of GAL4-VP16 binding.

1.3-, and 1.0-fold, respectively, in the presence of GAL4-VP16 and PC4 (Fig. 2), demonstrating that TAFs are essential for stimulating all of the steps, including initiation, promoter escape, and elongation, at least under the present assay conditions. Together, these observations suggest that both TFIIA and TAFs are indispensable for PC4 to effect noticeable stimulation of promoter escape as well as initiation (probably via facilitated PIC assembly) in response to GAL4-VP16.

PC4 interacts with TFIIH and GAL4-VP16 via its coactivator domain. A previous study showed that TFIIH is required for the stimulation of promoter escape because of its ERCC3 helicase activity (10) in activated transcription by GAL4-VP16 and PC4. The fact that both PC4 and TFIIH are required simultaneously to facilitate promoter escape prompted us to examine a possible physical interaction between PC4 and TFIIH. To do this, we performed GST pull-down assays by using PC4 fused to the C terminus of GST, which was expressed in *E. coli* and retained on the glutathione-Sepharose resin. Since recombinant TFIIH has a FLAG tag at the C terminus of its MO15 subunit and GAL4-VP16 has an N-terminal FLAG tag, both proteins were detected by Western blotting with anti-FLAG M2 antibody after separation by SDS-PAGE. As shown in Fig. 3A, TFIIH was found to bind to GST-PC4 but not to GST alone, indicating that PC4 interacts with TFIIH specifically. The interaction between PC4 and TFIIH seemed as strong as the well-characterized interaction between PC4 and VP16 (Fig. 3A) and that between TFIIH and the VP16 activation domain (Fig. 3B), since similar proportions (~10%) of input TFIIH and GAL4-VP16 were bound to GST-PC4 under the same conditions.

To explore the relevance of the interactions of PC4 with TFIIH and with GAL4-VP16 for the coactivator activity of PC4, we localized the region of PC4 that interacted with TFIIH and GAL4-VP16. We created N-terminal and C-terminal deletion mutants of PC4, as shown in Fig. 4A, and tested their interactions with TFIIH and GAL4-VP16. As shown in Fig. 4B and also summarized in Fig. 4A, the mutants PC4(22-127), PC4(43-127), PC4(63-127), PC4(1-62), and PC4(1-42) interacted with both TFIIH and GAL4-VP16, whereas PC4(92-127), PC4(107-127), and PC4(1-21) did not interact with either TFIIH or GAL4-VP16 (Fig. 4A and B), showing that PC4 interacts with TFIIH and GAL4-VP16 through the region from residue 22 to residue 91, a domain necessary and sufficient for the coactivator activity of PC4 (21, 27). Furthermore, the PC4 mutants PC4(1-62) and PC4(63-127), which do

not overlap with each other, interacted with both TFIIH and GAL4-VP16, suggesting that these interactions occur redundantly at multiple sites within the coactivator domain of PC4. The interactions of the different PC4 mutants with GAL4-VP16 were equally strong, whereas those with TFIIH showed variations; for example, PC4(43-127) interacted with TFIIH more strongly than wild-type PC4 did, while PC4(22-127), PC4(1-62), and PC4(1-42) interacted with TFIIH more weakly than wild-type PC4 did (Fig. 4B).

Thus, colocalization of the interaction region to the functionally defined coactivator domain (21, 27) argues that these interactions are functionally relevant for the coactivator activity of PC4. Moreover, the redundancy of these interactions is consistent with the role of PC4 as a coactivator, which is expected to interact with activators and the basal transcriptional machinery at the same time.

Distinct regulation of the interactions of PC4 with GAL4-VP16 and TFIIH. Since the interaction of TFIIH with PC4 mutants appeared to differ slightly from that of GAL4-VP16, we further explored the difference between these two interactions. The interaction between PC4 and GAL4-VP16 was previously shown to be negatively regulated by phosphorylation of the N-terminal region of PC4 (14, 27); therefore, we sought to determine whether the same was true for the interaction between PC4 and TFIIH. To make this determination, we used PC4-GST, in which the C terminus of PC4 is fused to the N terminus of GST, since GST-PC4 could not be phosphorylated efficiently by casein kinase II, presumably because the N-terminal phosphorylation sites of PC4 within GST-PC4 were sterically inaccessible to the casein kinase II (Fig. 5C). PC4-GST, expressed in *E. coli* and retained on glutathione-Sepharose, showed essentially the same binding to TFIIH and GAL4-VP16 as GST-PC4 did (data not shown). As shown in Fig. 5B, PC4-GST could be readily phosphorylated, and the phosphorylation slowed the migration of PC4-GST on the SDS gel, a shift of migration similar to that observed for nonfused PC4 (Fig. 5A), indicating that PC4-GST was phosphorylated in essentially the same manner as PC4 was. Pull-down assays with PC4-GST indicated not only that TFIIH interacted with both phosphorylated and nonphosphorylated PC4, but also that its interaction with PC4 was slightly enhanced by the phosphorylation of PC4 (Fig. 5D). In marked contrast, the interaction between GAL4-VP16 and PC4 was completely abolished upon phosphorylation of PC4, as reported previously (13, 27). Thus, although TFIIH and GAL4-VP16 interact with PC4 through the same coactivator domain, these interactions show markedly distinct regulation through the phosphorylation of PC4.

The number of GAL4 binding sites determines the degree to which each step of the transcriptional process is stimulated upon activation. The multiple interactions of GAL4-VP16 and PC4 with the basal transcription machinery, as demonstrated here and elsewhere, and the observed stimulatory effects before and after initiation suggest that each GAL4-VP16 dimer bound to the five GAL4 sites may have a distinct role in activated transcription. To gain further insight into a potential relationship between each GAL4-VP16 dimer and the effects on distinct steps, as well as the role of PC4 in this process, we determined the degree to which each step of transcription is stimulated in the presence and absence of PC4 when the number of bound GAL4-VP16 dimers was reduced (Fig. 6A). To

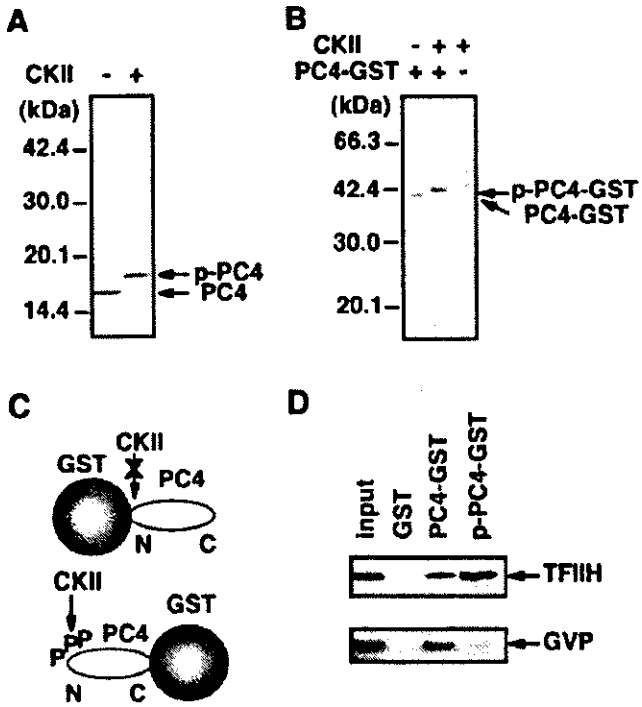

FIG. 5. PC4 interacts with TFIIH in a manner distinct from that of GAL4-VP16. (A) Phosphorylation of PC4 with casein kinase II (CKII). Purified PC4 was phosphorylated by casein kinase II (New England Biolabs), and the shifted mobility of PC4 was observed upon phosphorylation. The positions of phosphorylated PC4 (p-PC4) and nonphosphorylated PC4 (PC4) are shown on the right. (B) Phosphorylation of PC4-GST. The positions of phosphorylated PC4-GST (p-PC4-GST) and nonphosphorylated PC4-GST (PC4-GST) are indicated on the right. (C) As shown schematically, PC4 fused to the N terminus of GST was efficiently phosphorylated by casein kinase II. Casein kinase II phosphorylated PC4 fused to the N terminus, but not to the C terminus, of GST (data not shown), presumably because the phosphorylation sites within the N-terminal region of PC4 were sterically masked by GST. A GST molecule and PC4 are schematically represented, and a phosphate molecule and the amino and carboxyl termini of PC4 are indicated by P, N, and C, respectively. (D) Interaction of phosphorylated PC4 with TFIIH. GST pull-down assays with PC4-GST revealed that TFIIH interacted with both nonphosphorylated and phosphorylated forms of PC4 but that GAL4-VP16 interacted only with the nonphosphorylated form of PC4. Note that approximately twofold more TFIIH bound to p-PC4-GST than to PC4-GST.

this end, we created the templates with one, three, and five GAL4-binding sites (G1, G3, and G5 templates, respectively, binding 2, 6, and 10 GAL4-VP16 dimers) (Fig. 6A) and performed in vitro transcription analyses. As shown in Fig. 6 and quantified in Fig. 7, GAL4-VP16 alone stimulated the level of the 390-nt transcripts from the G1, G3, and G5 templates 2.6-, 2.9-, and 3.5-fold, respectively, showing that increasing the number of bound GAL4-VP16 dimers does not necessarily lead to robust transcriptional activation when PC4 is absent from the reactions. In the presence of PC4, however, stimulation of the 390-nt transcript increased dramatically to 5.3-, 14.3-, and 17.2-fold for the G1, G3, and G5 templates, respectively (Fig. 6B and 7A), revealing that the effect of PC4 becomes more apparent as the number of GAL4-VP16 dimers is increased. Moreover, DNase I footprint analyses showed that

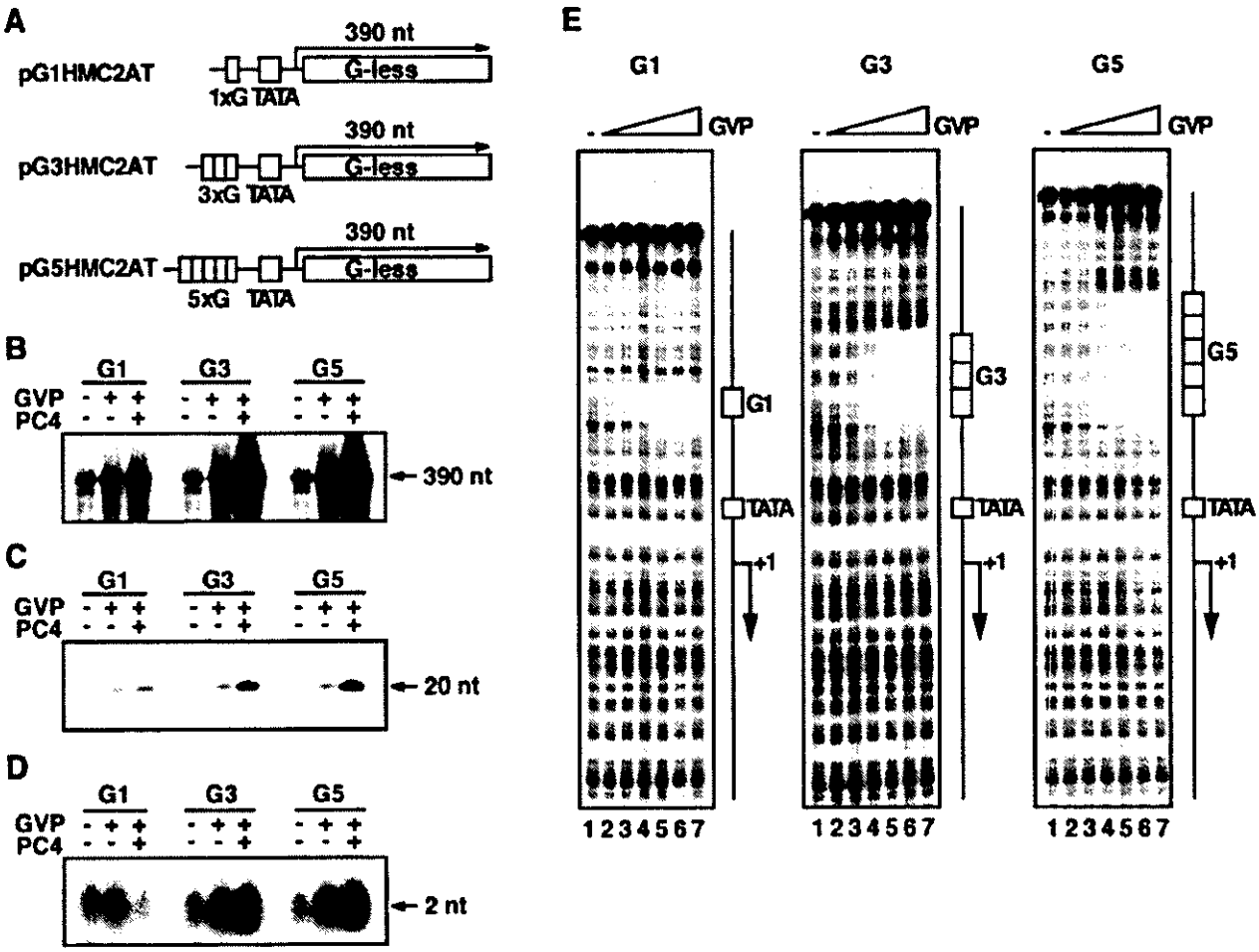

FIG. 6. Effect of the number of GAL4 sites on the degree of stimulation of the 390-, 20-, and 2-nt transcripts. (A) Templates used for in vitro transcription. Three templates, pG1HMC2AT, pG3HMC2AT, and pG5HMC2AT, contained one, three, and five GAL4 binding sites, respectively. For in vitro transcription for 20-nt transcripts, the same set of the templates with a G residue at the +20 position (not shown) was used. The amount of GAL4-VP16 added to the transcription reaction was the same for all reactions (25 ng). (B to D) The effects of one, three, and five GAL4 sites on the stimulation of the 390-nt (B), 20-nt (C), and 2-nt (D) transcripts. G1, G3, and G5 indicate pG1HMC2AT, pG3HMC2AT, and pG5HMC2AT, respectively. (E) Binding of GAL4-VP16 to the G1, G3, and G5 templates. Increasing amounts of GAL4-VP16 were tested for binding to the DNA fragments containing one, three, and five GAL4 sites. The added amounts of GAL4-VP16 were 0 ng (lane 1), 1.6 ng (lane 2), 3.1 ng (lane 3), 6.3 ng (lane 4), 12.5 ng (lane 5), 25 ng (lane 6), and 50 ng (lane 7). The positions of GAL4 binding sites (G1, G3, and G5), the TATA box (TATA), and the initiation site (+1) are indicated on the right.

all of the GAL4 sites on the G1, G3, and G5 templates were occupied almost completely by 25 ng of GAL4-VP16 (Fig. 6E, lane 6), the amount that was used for in vitro transcription reactions. Thus, it is unlikely that transcriptional activation for the G3 and G5 templates derives from the PC4-induced cooperative binding of GAL4-VP16 to its cognate sites. More likely, however, is the possibility that PC4 increases the number, or the effectiveness, of the interactions between GAL4-VP16 and the basal transcription machinery to allow synergistic effects of multiply bound GAL4-VP16 dimers (Fig. 7A).

Next, to determine the relative stimulation of initiation, promoter escape, and elongation in activated transcription from the G1, G3, and G5 templates, we assayed and quantified the amounts of the 2- and 20-nt transcripts from these templates (Fig. 6C and D) and then ascribed the effects of GAL4-VP16 or of GAL4-VP16 and PC4 to three distinct steps (Fig. 7B and C). The analyses of the transcripts from the G1 template in the presence of GAL4-VP16 alone revealed minor stimulation of initiation, with little stimulation of promoter escape and elongation. However, markedly increased levels of stimulation of promoter escape and, to a lesser extent, elongation were observed when PC4 was included in these reactions (Fig. 7C, top panel). Interestingly, no stimulation whatsoever of initiation from the G1 template was observed in the presence of both GAL4-VP16 and PC4 (Fig. 7C, top panel). In contrast, robust activation of transcription from the G3 and G5 templates by GAL4-VP16 and PC4 was attributed largely to the marked stimulation of both initiation and promoter escape (Fig. 7C, middle and bottom panels). Low levels of transcriptional activation for these templates in the presence of GAL4-VP16 alone, however, resulted mainly from the stimulation of initiation.

These data demonstrate the following points. First, GAL4-VP16 alone can effect a low level of stimulation of the initia-

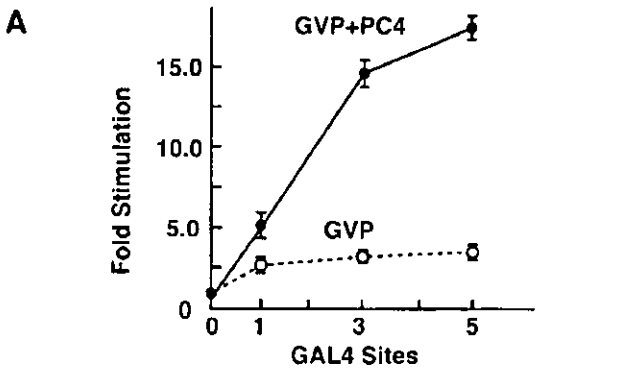

B

Transcript		Fold Stimulation	
		+GVP	+GVP, +PC4
G1	2 nt	1.5 ± 0.1	0.9 ± 0.1
	20 nt	2.0 ± 0.3	2.5 ± 0.4
	390 nt	2.6 ± 0.2	5.3 ± 1.8
G3	2 nt	2.1 ± 0.3	2.8 ± 0.2
	20 nt	2.8 ± 0.2	10.2 ± 0.9
	390 nt	2.9 ± 0.1	14.3 ± 1.8
G5	2 nt	2.0 ± 0.4	3.2 ± 0.2
	20 nt	2.5 ± 0.5	10.1 ± 2.4
	390 nt	3.5 ± 0.2	17.2 ± 1.7

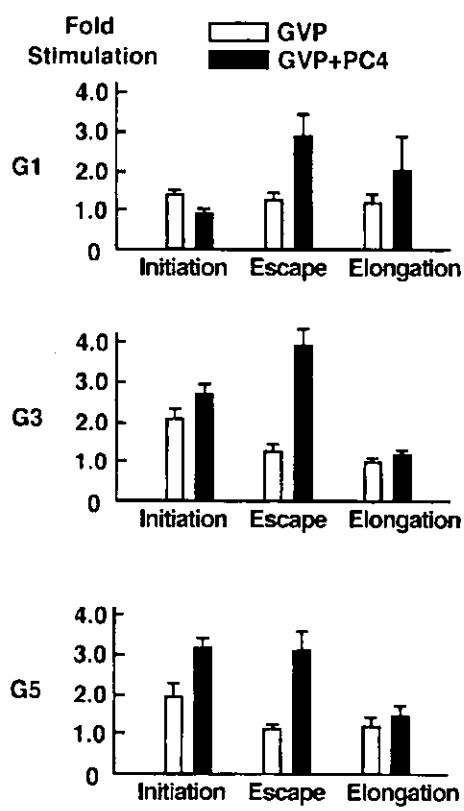

FIG. 7. The stimulation of initiation, promoter escape, and elongation on the templates with different numbers of GAL4-sites. (A) The effect of coactivation by PC4 became more pronounced as the number of GAL4 sites was increased. The levels of the 390-nt transcripts shown in Fig. 6 were quantified by using Fujix BAS 2000, and the values of stimulation (n-fold) were calculated. The standard deviations for three independent experiments are indicated. (B) The values of activation (n-fold) for the 2-, 20-, and 390-nt transcripts were determined from three independent experiments and are shown as means ± standard deviations. (C) The number of GAL4 sites influences the activation of initiation, promoter escape, and elongation. The values for stimulation (n-fold) of initiation, promoter escape, and elongation were calculated as those presented in Fig. 1 were. On the templates with a single GAL4 site, PC4 stimulated promoter escape rather than initiation of GAL4-VP16-dependent transcription, while on the templates with three or five GAL4 sites, PC4 stimulated both initiation and promoter escape to similar extents. There were small but reproducible effects on elongation in all experiments.

tion step but little, if any, promoter escape, regardless of the number of its binding sites. Second, PC4 increases the degrees to which GAL4-VP16 stimulates initiation and promoter escape, having a more pronounced effect on promoter escape than on initiation. Third, promoter escape appears to be preferentially stimulated by GAL4-VP16 in the presence of PC4 when GAL4-VP16 is bound on a single GAL4 site. Together, these observations suggest that each GAL4-VP16 dimer bound on the promoter may stimulate a distinct step of transcription.

DISCUSSION

Although a large body of evidence indicates the functional significance of coactivators in regulating transcription in vitro and in vivo (2, 18, 20, 36, 41), far less is known about the precise mechanism(s) by which these coactivators stimulate transcription in conjunction with activators, especially in the context of naked DNA templates. In the present study, we took advantage of a well-defined reconstituted in vitro transcription system (10, 12) and demonstrated a crucial role for a coactivator, PC4, in stimulating promoter escape in activated transcription, in part through direct interaction with TFIIH.

Figure 8 depicts how PC4 enables GAL4-VP16 to achieve a high level of transcriptional activation. This model postulates at least two targets, termed targets A and B, in the basal transcription machinery, to which signals from activators are transmitted. These signals, in turn, permit target A and target B to regulate the steps leading to initiation (PIC assembly, promoter opening, and initiation) and promoter escape, respectively. Each target postulated in the model is meant to represent multiple factors rather than a single factor, and, conversely, a single factor may constitute a part of more than one target. For instance, since TFIIA and TFIID are important for facilitating both PIC assembly (7, 8, 24, 25) and promoter escape (Fig. 2), each factor must constitute parts of both target A and target B. In addition, PC4 and TFIIH (Fig. 3, 4, and 5), whose ERCC3 helicase activity is also essential for stimulating promoter escape (10), are likely to constitute the target B that regulates promoter escape. This complex network of multiple interactions may induce conformational changes, including

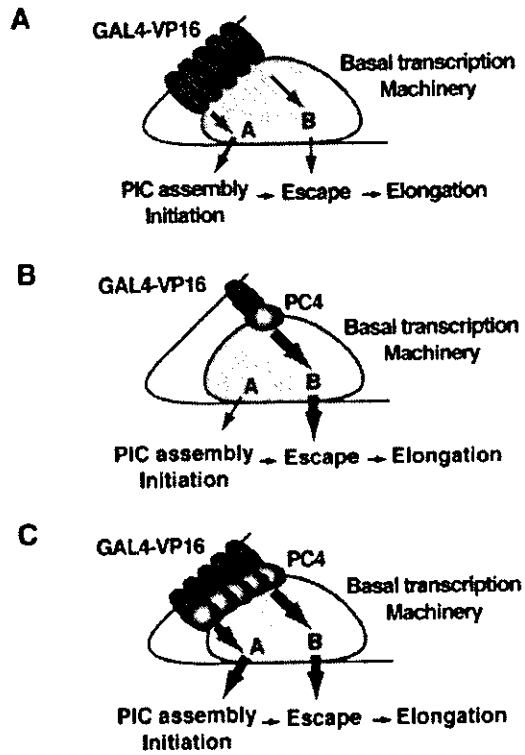

FIG. 8. A model of PC4 coactivator activity. In this model, we postulate that the basal transcription machinery contains at least two targets, termed targets A and B, through which the signals from activators are transmitted either directly or via PC4 to the individual steps of the transcription process. Target A regulates the steps leading to initiation (PIC assembly, promoter opening, and initiation) and is likely to consist of more discrete targets, whereas target B regulates promoter escape. (A) In the absence of PC4, GAL4-VP16 elicits transcriptional activation through the predominant effect on target A, regardless of the number of bound GAL4-VP16 molecules. (B) When PC4 is present, GAL4-VP16 bound at a single GAL4 site provides substantial transcriptional activation through target B. (C) When PC4 is present, multiply bound GAL4-VP16 achieves robust transcription through the synergized effects on both target A and target B, enhanced by PC4.

isomerization of the DA complex (7), that lead to stimulation of individual steps of the transcriptional process.

In the absence of PC4, GAL4-VP16 appears to function mainly through target A, and even increasing the number of GAL4-VP16 dimers bound on the template does not lead to robust transcriptional activation (Fig. 8A). In the presence of PC4, however, GAL4-VP16 can function through target B and also augment the effect through target A. Of the two postulated targets, target B seems to be preferred by the combination of GAL4-VP16 and PC4, since PC4 directs GAL4-VP16 to function predominantly through target B when the amount of GAL4-VP16 is limited, as on the G1 template (Fig. 8B). In contrast, when multiply bound GAL4-VP16 dimers are present, as on the G3 and G5 templates, PC4 permits distinct GAL4-VP16 molecules to function through both target A and target B (Fig. 8C), providing a mechanism for transcriptional synergy (6, 17, 34, 35, 46).

In this model, it is implicitly assumed that GAL4-VP16 and PC4 are capable of multiple interactions with the basal transcription machinery, interactions that obligate GAL4-VP16 and PC4 to adopt different conformations depending upon the target to which they bind. This assumption is supported not only by numerous interaction studies but also by recent structural studies showing that transcriptional activation domains, including that of VP16, are poorly structured in their free form but undergo an induced structural transition when complexed with their targets (5, 9, 30, 45, 51–53, 57, 61). In addition, the VP16 activation domain can adopt different structures whether it is bound to TBP or TFIIB (53). Moreover, this structural flexibility is also displayed by a mediator-like coactivator complex, CSRP (42, 56). Thus, given the lack of a stable three-dimensional structure within its coactivator domain (3), PC4 may form a stable structure only upon binding to activators and the basal transcription machinery. Through these interactions, PC4 could bestow activators with extra surfaces and an added conformational flexibility that permit more functionally effective links between activators and the basal transcription machinery.

Our model of PC4 action appears to contradict the widely accepted notion that PIC assembly is the primary target for activated transcription, as demonstrated by various in vivo and in vitro studies (47). In particular, using a similar in vitro transcription system, Chi et al. (7, 8) demonstrated that PIC assembly, especially DA complex assembly, is necessary and sufficient for activation, an observation supported by others (24, 25, 54, 55). Furthermore, Jacob and Luse (19) failed to detect any stimulatory effect on promoter escape by GAL4-VP16 by using HeLa nuclear extract. We believe, however, that this apparent contradiction can be reconciled for the following reasons. First, the effect on PIC assembly as inferred by the order-of-addition experiments does not necessarily dictate the actual time point at which the assembled PIC acts on steps of transcription. Thus, the effects of the assembled PIC, such as the isomerized DA complex (7), may remain far beyond the time point of their assembly. Second, we also observed the predominant effects on initiation (which may reflect PIC assembly in our assays) to overall stimulation of transcription when the amounts of factors were reduced. We suspect that, under these conditions, the stimulatory effect on promoter escape may be easily overlooked. Third, since PC4 acts as a coactivator only in its nonphosphorylated form (14, 27) and also in a highly concentration-dependent manner (13), PC4 may not have been functional as a coactivator in the transcription systems involving crude fractions (7, 8, 19, 24, 25), in which the majority of PC4 is phosphorylated (14, 27). Given these considerations, our results are not inconsistent with earlier observations that emphasized the predominant role of PIC assembly in transcriptional activation.

The exact mechanism by which PC4 assists the ERCC3 helicase of TFIIH during promoter escape remains an enigma. One attractive possibility is that PC4 stabilizes the ssDNA region exposed during promoter escape through its ssDNA-binding ability (62), thereby indirectly assisting the ERCC3 helicase. It is generally known that ssDNA-binding proteins stimulate the activities of DNA polymerases and helicases (7), and indeed, PC4 facilitates DNA replication mediated by SV40 T antigen (44). However, the possibility of this mechanism seems remote because a PC4 mutant, W89A, which has little ssDNA-binding ability (63), shows essentially the same effect

on promoter escape as wild-type PC4 does (10). Therefore, we favor alternative mechanisms by which PC4 facilitates the recruitment of TFIIH (29) or directly stabilizes the ATP-induced conformational change of TFIIH per se through protein-protein interactions, a mechanism consistent with the fact that TFIIH does not function as a classical helicase (22). Related to this idea, HBx, a coactivator-like transcriptional regulator of the hepatitis B virus (15), stimulates TFIIH helicase activities independently of its ssDNA-binding ability (48).

In conclusion, we have shown that PC4 assists GAL4-VP16 in stimulating the multiple steps of transcription and facilitates synergy by multiply bound GAL4-VP16 dimers. Future studies should address more detailed mechanistic aspects of the coactivator activity of PC4 and identify the precise factors within the basal transcription machinery that are targeted by individual GAL4-VP16 and PC4 molecules bound multiply on a single promoter. These studies may offer a paradigm for further functional analyses of diverse coactivators.

ACKNOWLEDGMENTS

We thank K. Nakagawa and Y. Miyagi for technical assistance and other members of the laboratory for materials, advice, discussion, and critical reading of the manuscript.

This study was supported by grants-in-aid from the Ministry of Education, Science, Sports and Culture, by the Maruki Memorial Prize of Saitama Medical School, and by a grant from the Sumitomo Foundation. A.F. was a Research Fellow of the Japan Society for the Promotion of Science.

REFERENCES

1. **Akhtar, A., G. Faye, and D. L. Bentley.** 1996. Distinct activated and non-activated RNA polymerase II complexes in yeast. EMBO J. **15**:4654–4664.
2. **Berk, A. J.** 1999. Activation of RNA polymerase II transcription. Curr. Opin. Cell Biol. **11**:330–335.
3. **Brandsen, J., S. Werten, P. C. van der Vliet, M. Meisterernst, J. Kroon, and P. Gros.** 1997. C-terminal domain of transcription cofactor PC4 reveals dimeric ssDNA binding site. Nat. Struct. Biol. **4**:900–903.
4. **Brown, C. E., T. Lechner, L. Howe, and J. L. Workman.** 2000. The many HATs of transcription coactivators. Trends Biochem. Sci. **25**:15–19.
5. **Campbell, K. M., A. R. Terrell, P. J. Laybourn, and K. J. Lumb.** 2000. Intrinsic structural disorder of the C-terminal activation domain from the bZIP transcription factor Fos. Biochemistry **39**:2708–2713.
6. **Carey, M., Y. S. Lin, M. R. Green, and M. Ptashne.** 1990. A mechanism for synergistic activation of a mammalian gene by GAL4 derivatives. Nature **345**:361–364.
7. **Chi, T., and M. Carey.** 1996. Assembly of the isomerized TFIIA-TFIID-TATA ternary complex is necessary and sufficient for gene activation. Genes Dev. **10**:2540–2550.
8. **Chi, T., P. Lieberman, K. Ellwood, and M. Carey.** 1995. A general mechanism for transcriptional synergy by eukaryotic activators. Nature **377**:254–257.
9. **Dahlman-Wright, K., H. Baumann, I. J. McEwan, T. Almlof, A. P. Wright, J. A. Gustafsson, and T. Hard.** 1995. Structural characterization of a minimal functional transactivation domain from the human glucocorticoid receptor. Proc. Natl. Acad. Sci. USA **92**:1699–1703.
10. **Fukuda, A., Y. Nogi, and K. Hisatake.** 2002. The regulatory role for the ERCC3 helicase of general transcription factor TFIIH during promoter escape in transcriptional activation. Proc. Natl. Acad. Sci. USA **99**:1206–1211.
11. **Fukuda, A., S. Tokonabe, M. Hamada, M. Matsumoto, T. Tsukui, Y. Nogi, and K. Hisatake.** 2003. Alleviation of PC4-mediated transcriptional repression by the ERCC3 helicase activity of general transcription factor TFIIH. J. Biol. Chem. **278**:14827–14831.
12. **Fukuda, A., J. Yamauchi, S. Y. Wu, C. M. Chiang, M. Muramatsu, and K. Hisatake.** 2001. Reconstitution of recombinant TFIIH that can mediate activator-dependent transcription. Genes Cells **6**:707–719.
13. **Ge, H., and R. G. Roeder.** 1994. Purification, cloning, and characterization of a human coactivator, PC4, that mediates transcriptional activation of class II genes. Cell **78**:513–523.
14. **Ge, H., Y. Zhao, B. T. Chait, and R. G. Roeder.** 1994. Phosphorylation negatively regulates the function of coactivator PC4. Proc. Natl. Acad. Sci. USA **91**:12691–12695.
15. **Haviv, I., D. Vaizel, and Y. Shaul.** 1996. pX, the HBV-encoded coactivator, interacts with components of the transcription machinery and stimulates transcription in a TAF-independent manner. EMBO J. **15**:3413–3420.
16. **Henry, N. L., D. A. Bushnell, and R. D. Kornberg.** 1996. A yeast transcriptional stimulatory protein similar to human PC4. J. Biol. Chem. **271**:21842–21847.
17. **Hori, R., and M. Carey.** 1994. The role of activators in assembly of RNA polymerase II transcription complexes. Curr. Opin. Genet. Dev. **4**:236–244.
18. **Ito, M., and R. G. Roeder.** 2001. The TRAP/SMCC/Mediator complex and thyroid hormone receptor function. Trends Endocrinol. Metab. **12**:127–134.
19. **Jacob, G. A., and D. S. Luse.** 1996. GAL4-VP16 stimulates two RNA polymerase II promoters primarily at the preinitiation complex assembly step. Gene Expr. **5**:193–203.
20. **Kaiser, K., and M. Meisterernst.** 1996. The human general co-factors. Trends Biochem. Sci. **21**:342–345.
21. **Kaiser, K., G. Stelzer, and M. Meisterernst.** 1995. The coactivator p15 (PC4) initiates transcriptional activation during TFIIA-TFIID-promoter complex formation. EMBO J. **14**:3520–3527.
22. **Kim, T. K., R. H. Ebright, and D. Reinberg.** 2000. Mechanism of ATP-dependent promoter melting by transcription factor IIH. Science **288**:1418–1422.
23. **Knaus, R., R. Pollock, and L. Guarente.** 1996. Yeast SUB1 is a suppressor of TFIIB mutations and has homology to the human co-activator PC4. EMBO J. **15**:1933–1940.
24. **Kobayashi, N., T. G. Boyer, and A. J. Berk.** 1995. A class of activation domains interacts directly with TFIIA and stimulates TFIIA-TFIID-promoter complex assembly. Mol. Cell. Biol. **15**:6465–6473.
25. **Kobayashi, N., P. J. Horn, S. M. Sullivan, S. J. Triezenberg, T. G. Boyer, and A. J. Berk.** 1998. DA-complex assembly activity required for VP16C transcriptional activation. Mol. Cell. Biol. **18**:4023–4031.
26. **Kraus, W. L., and J. T. Kadonaga.** 1998. p300 and estrogen receptor cooperatively activate transcription via differential enhancement of initiation and reinitiation. Genes Dev. **12**:331–342.
27. **Kretzschmar, M., K. Kaiser, F. Lottspeich, and M. Meisterernst.** 1994. A novel mediator of class II gene transcription with homology to viral immediate-early transcriptional regulators. Cell **78**:525–534.
28. **Krumm, A., L. B. Hickey, and M. Groudine.** 1995. Promoter-proximal pausing of RNA polymerase II defines a general rate-limiting step after transcription initiation. Genes Dev. **9**:559–572.
29. **Kumar, K. P., S. Akoulitchev, and D. Reinberg.** 1998. Promoter-proximal stalling results from the inability to recruit transcription factor IIH to the transcription complex and is a regulated event. Proc. Natl. Acad. Sci. USA **95**:9767–9772.
30. **Lee, H., K. H. Mok, R. Muhandiram, K. H. Park, J. E. Suk, D. H. Kim, J. Chang, Y. C. Sung, K. Y. Choi, and K. H. Han.** 2000. Local structural elements in the mostly unstructured transcriptional activation domain of human p53. J. Biol. Chem. **275**:29426–29432.
31. **Lee, Y. C., J. M. Park, S. Min, S. J. Han, and Y. J. Kim.** 1999. An activator binding module of yeast RNA polymerase II holoenzyme. Mol. Cell. Biol. **19**:2967–2976.
32. **Lemon, B., and R. Tjian.** 2000. Orchestrated response: a symphony of transcription factors for gene control. Genes Dev. **14**:2551–2569.
33. **Lieberman, P. M., J. Ozer, and D. B. Gursel.** 1997. Requirement for transcription factor IIA (TFIIA)-TFIID recruitment by an activator depends on promoter structure and template competition. Mol. Cell. Biol. **17**:6624–6632.
34. **Lin, Y. S., M. Carey, M. Ptashne, and M. R. Green.** 1990. How different eukaryotic transcriptional activators can cooperate promiscuously. Nature **345**:359–361.
35. **Lin, Y. S., and M. R. Green.** 1991. Mechanism of action of an acidic transcriptional activator in vitro. Cell **64**:971–981.
36. **Malik, S., and R. G. Roeder.** 2000. Transcriptional regulation through Mediator-like coactivators in yeast and metazoan cells. Trends Biochem. Sci. **25**:277–283.
37. **Malik, S., A. E. Wallberg, Y. K. Kang, and R. G. Roeder.** 2002. TRAP/SMCC/mediator-dependent transcriptional activation from DNA and chromatin templates by orphan nuclear receptor hepatocyte nuclear factor 4. Mol. Cell. Biol. **22**:5626–5637.
38. **Meisterernst, M., A. L. Roy, H. M. Lieu, and R. G. Roeder.** 1991. Activation of class II gene transcription by regulatory factors is potentiated by a novel activity. Cell **66**:981–993.
39. **Moqtaderi, Z., Y. Bai, D. Poon, P. A. Weil, and K. Struhl.** 1996. TBP-associated factors are not generally required for transcriptional activation in yeast. Nature **383**:188–191.
40. **Myers, L. C., and R. D. Kornberg.** 2000. Mediator of transcriptional regulation. Annu. Rev. Biochem. **69**:729–749.
41. **Naar, A. M., B. D. Lemon, and R. Tjian.** 2001. Transcriptional coactivator complexes. Annu. Rev. Biochem. **70**:475–501.
42. **Naar, A. M., D. J. Taatjes, W. Zhai, E. Nogales, and R. Tjian.** 2002. Human CRSP interacts with RNA polymerase II CTD and adopts a specific CTD-bound conformation. Genes Dev. **16**:1339–1344.
43. **Oelgeschlager, T., Y. Tao, Y. K. Kang, and R. G. Roeder.** 1998. Transcription activation via enhanced preinitiation complex assembly in a human cell-free system lacking TAFIIs. Mol. Cell **1**:925–931.

44. **Pan, Z. Q., H. Ge, A. A. Amin, and J. Hurwitz.** 1996. Transcription-positive cofactor 4 forms complexes with HSSB (RPA) on single-stranded DNA and influences HSSB-dependent enzymatic synthesis of simian virus 40 DNA. J. Biol. Chem. **271**:22111–22116.
45. **Parker, D., U. S. Jhala, I. Radhakrishnan, M. B. Yaffe, C. Reyes, A. L. Shulman, L. C. Cantley, P. E. Wright, and M. Montminy.** 1998. Analysis of an activator:coactivator complex reveals an essential role for secondary structure in transcriptional activation. Mol. Cell **2**:353–359.
46. **Ptashne, M.** 1988. How eukaryotic transcriptional activators work. Nature **335**:683–689.
47. **Ptashne, M., and A. Gann.** 1997. Transcriptional activation by recruitment. Nature **386**:569–577.
48. **Qadri, I., J. W. Conaway, R. C. Conaway, J. Schaack, and A. Siddiqui.** 1996. Hepatitis B virus transactivator protein, HBx, associates with the components of TFIIH and stimulates the DNA helicase activity of TFIIH. Proc. Natl. Acad. Sci. USA **93**:10578–10583.
49. **Roeder, R. G.** 1998. Role of general and gene-specific cofactors in the regulation of eukaryotic transcription. Cold Spring Harb. Symp. Quant. Biol. **63**:201–218.
50. **Roeder, R. G.** 1996. The role of general initiation factors in transcription by RNA polymerase II. Trends Biochem. Sci. **21**:327–335.
51. **Schmitz, M. L., M. A. dos Santos Silva, H. Altmann, M. Czisch, T. A. Holak, and P. A. Baeuerle.** 1994. Structural and functional analysis of the NF-kappa B p65 C terminus. An acidic and modular transactivation domain with the potential to adopt an alpha-helical conformation. J. Biol. Chem. **269**:25613–25620.
52. **Shen, F., S. J. Triezenberg, P. Hensley, D. Porter, and J. R. Knutson.** 1996. Critical amino acids in the transcriptional activation domain of the herpesvirus protein VP16 are solvent-exposed in highly mobile protein segments. An intrinsic fluorescence study. J. Biol. Chem. **271**:4819–4826.
53. **Shen, F., S. J. Triezenberg, P. Hensley, D. Porter, and J. R. Knutson.** 1996. Transcriptional activation domain of the herpesvirus protein VP16 becomes conformationally constrained upon interaction with basal transcription factors. J. Biol. Chem. **271**:4827–4837.
54. **Shykind, B. M., J. Kim, and P. A. Sharp.** 1995. Activation of the TFIID-TFIIA complex with HMG-2. Genes Dev. **9**:1354–1365.
55. **Shykind, B. M., J. Kim, L. Stewart, J. J. Champoux, and P. A. Sharp.** 1997. Topoisomerase I enhances TFIID-TFIIA complex assembly during activation of transcription. Genes Dev. **11**:397–407.
56. **Taatjes, D. J., A. M. Naar, F. Andel III, E. Nogales, and R. Tjian.** 2002. Structure, function, and activator-induced conformations of the CRSP coactivator. Science **295**:1058–1062.
57. **Uesugi, M., O. Nyanguile, H. Lu, A. J. Levine, and G. L. Verdine.** 1997. Induced alpha helix in the VP16 activation domain upon binding to a human TAF. Science **277**:1310–1313.
58. **Verrijzer, C. P., and R. Tjian.** 1996. TAFs mediate transcriptional activation and promoter selectivity. Trends Biochem. Sci. **21**:338–342.
59. **Walker, S. S., J. C. Reese, L. M. Apone, and M. R. Green.** 1996. Transcription activation in cells lacking TAFIIS. Nature **383**:185–188.
60. **Wang, W., M. Carey, and J. D. Gralla.** 1992. Polymerase II promoter activation: closed complex formation and ATP-driven start site opening. Science **255**:450–453.
61. **Warnmark, A., A. Wikstrom, A. P. Wright, J. A. Gustafsson, and T. Hard.** 2001. The N-terminal regions of estrogen receptor alpha and beta are unstructured in vitro and show different TBP binding properties. J. Biol. Chem. **276**:45939–45944.
62. **Werten, S., F. W. Langen, R. van Schaik, H. T. Timmers, M. Meisterernst, and P. C. van der Vliet.** 1998. High-affinity DNA binding by the C-terminal domain of the transcriptional coactivator PC4 requires simultaneous interaction with two opposing unpaired strands and results in helix destabilization. J. Mol. Biol. **276**:367–377.
63. **Werten, S., G. Stelzer, A. Goppelt, F. M. Langen, P. Gros, H. T. Timmers, P. C. Van der Vliet, and M. Meisterernst.** 1998. Interaction of PC4 with melted DNA inhibits transcription. EMBO J. **17**:5103–5111.
64. **Wu, S. Y., E. Kershnar, and C. M. Chiang.** 1998. TAFII-independent activation mediated by human TBP in the presence of the positive cofactor PC4. EMBO J. **17**:4478–4490.
65. **Xu, L., C. K. Glass, and M. G. Rosenfeld.** 1999. Coactivator and corepressor complexes in nuclear receptor function. Curr. Opin. Genet. Dev. **9**:140–147.
66. **Yankulov, K., J. Blau, T. Purton, S. Roberts, and D. L. Bentley.** 1994. Transcriptional elongation by RNA polymerase II is stimulated by transactivators. Cell **77**:749–759.
67. **Yudkovsky, N., J. A. Ranish, and S. Hahn.** 2000. A transcription reinitiation intermediate that is stabilized by activator. Nature **408**:225–229.

The EMBO Journal (2004) 23, 1075–1088 | © 2004 European Molecular Biology Organization | All Rights Reserved 0261-4189/04
www.embojournal.org

THE EMBO JOURNAL

Tiam1 mediates neurite outgrowth induced by ephrin-B1 and EphA2

Masamitsu Tanaka[1,2], Riuko Ohashi[1,3], Ritsuko Nakamura[1], Kazuya Shinmura[1], Takaharu Kamo[1], Ryuichi Sakai[2] and Haruhiko Sugimura[1,*]

[1]First Department of Pathology, Hamamatsu University School of Medicine, Handayama, Hamamatsu, Japan and [2]Growth Factor Division, National Cancer Center Research Institute, Tsukiji, Chuo-ku, Tokyo, Japan

Bidirectional signals mediated by Eph receptor tyrosine kinases and their membrane-bound ligands, ephrins, play pivotal roles in the formation of neural networks by induction of both collapse and elongation of neurites. However, the downstream molecular modules to deliver these cues are largely unknown. We report here that the interaction of a Rac1-specific guanine nucleotide-exchanging factor, Tiam1, with ephrin-B1 and EphA2 mediates neurite outgrowth. In cells coexpressing Tiam1 and ephrin-B1, Rac1 is activated by the extracellular stimulation of clustered soluble EphB2 receptors. Similarly, soluble ephrin-A1 activates Rac1 in cells coexpressing Tiam1 and EphA2. Cortical neurons from the E14 mouse embryos and neuroblastoma cells significantly extend neurites when placed on surfaces coated with the extracellular domain of EphB2 or ephrin-A1, which were abolished by the forced expression of the dominant-negative mutant of ephrin-B1 or EphA2. Furthermore, the introduction of a dominant-negative form of Tiam1 also inhibits neurite outgrowth induced by the ephrin-B1 and EphA2 signals. These results indicate that Tiam1 is required for neurite outgrowth induced by both ephrin-B1-mediated reverse signaling and EphA2-mediated forward signaling.

The EMBO Journal (2004) **23**, 1075–1088. doi:10.1038/sj.emboj.7600128; Published online 26 February 2004
Subject Categories: signal transduction; cell & tissue architecture
Keywords: cortical neuron; Eph; ephrin; neurite outgrowth; Tiam1

Introduction

The members of the Eph receptors and their ligands are variously involved in neural development: regulating axon guidance, axon fasciculation and synaptogenesis. The interaction of Eph and ephrin regulates axon guidance by a repulsive function. Retinal axons expressing EphA receptors are guided to their target tectal area according to interactions with a repellent ephrin-A gradient (Cheng *et al*, 1995). The pathfinding of mouse anterior commissure is also regulated by the repulsive function between ephrin-B1 and EphB2 receptor (Henkemeyer *et al*, 1996). On the other hand, the interaction of Eph and ephrin also induces attractive axon guidance in certain settings. Vomeronasal axons expressing ephrin-A5 are attractively elongated by interaction with target EphA receptors in the accessory olfactory bulb, implying that ephrin-A mediates attractive guidance mechanisms (Knoll *et al*, 2001). Another example of attractive axon guidance is also reported in terms of the interaction of the EphB receptor and ephrin-B. Mann *et al* (2002) show that *Xenopus* dorsal retinal axons expressing ephrin-B preferentially project to the tectal area where EphB1 is highly expressed, while the ventral ones that express EphB2 project to the dorsal area of the tectum where ephrin-Bs are highly expressed. Therefore, Eph receptors and ephrins are involved in both repulsive and attractive guidance mechanisms during the establishment of neuronal connections. Gao *et al* have previously shown the two opposing effects of Eph receptors and ephrins on neurite outgrowth *in vitro* by a series of experiments. Primary cultured rat neurons extended or retracted neurites when they were plated on cells stably expressing various Eph or ephrins on their surface (Gao *et al*, 1996, 1998, 1999, 2000). However, the molecular basis of such morphological change requires investigation.

Rho GTPases are important regulators of the actin cytoskeleton. Activation of RhoA and its effector protein Rho-kinase (ROCK) leads to growth cone collapse, neurite retraction or neurite growth inhibition by inducing the contraction of actomyosin (Wahl *et al*, 2000). On the other hand, activation of Rac1 induces neurite elongation. Tiam1, a specific guanine-nucleotide exchange factor (GEF) for Rac1 (Habets *et al*, 1994), affects neuronal morphology (Leeuwen *et al*, 1997; Kunda *et al*, 2001). Moreover, STEF, another GEF for Rac1, which has highly homologous regions with Tiam1, is also effective in neurite outgrowth (Matsuo *et al*, 2002). The cellular localization of Tiam1 and EphA2 is similar. When cells were cultured sparsely, both EphA2 and activated Tiam1 are highly expressed at the cell periphery containing membrane ruffles. However, when cells were adhered to each other, they are highly expressed at the site of cell-to-cell adhesion (Sander *et al*, 1998; Zantek *et al*, 1999). These observations led us to focus on the examination whether Tiam1 and EphA2 interact, and Tiam1 could be a mediator of EphA2 receptor. During the examination of the interaction of Tiam1 with several Eph receptors and ephrins, we have found that ephrin-B1 also associates with Tiam1.

In this study, we describe the interaction of Tiam1 with ephrin-B1 and EphA2. A part of Tiam1 was accumulated to the sites including clustered ephrin-B1 and EphA2 after the

*Corresponding author. First Department of Pathology, Hamamatsu University School of Medicine, 1-20-1 Handayama, Hamamatsu 431-3192, Japan. Tel.: +81 53 435 2220; Fax: +81 53 435 2225; E-mail: hsugimur@hama-med.ac.jp
[3]Present address: Division of Cellular and Molecular Pathology, Department of Cellular Function, Niigata University Graduate School of Medical and Dental Sciences, Asahimachi-dori 1, Niigata 951-8510, Japan

Received: 9 April 2003; accepted: 19 January 2004; published online: 26 February 2004

cells were stimulated with EphB2 and ephrin-A1, respectively. Neurite outgrowth was observed in primary cortical neurons from mouse embryos in response to the stimulation of EphB2-Fc, and NB1 neuroblastoma cells in response to ephrin-a1-Fc. Coexpression of the dominant-negative mutant of Tiam1, or mutant of ephrin-B1 or EphA2, which lacks its cytoplasmic region prevented the neurite extension described above. These results suggest that Tiam1 is a mediator of ephrin-B1- and EphA2-induced neurite outgrowth.

Results

Tiam1 interacts with the cytoplasmic domain of ephrin-B1 and EphA2

We have examined the association between Tiam1 with ephrin-B1 and EphA2 *in vivo*. Coexpression and co-precipitation analysis in COS1 cells revealed that Tiam1 was co-precipitated with ephrin-B1 and EphA2 by specific antibodies (Figure 1A, lanes 1 and 3, arrowheads, respectively), but not by the normal goat serum or mouse IgG1 (Figure 1A, lanes 2 and 4, arrowheads, respectively). These results were further confirmed by experiments using the antibodies in reverse order. Ephrin-B1 and EphA2 were co-precipitated with Tiam1 (Figure 1A, lanes 5 and 7, arrowheads, respectively). Next, we have generated several truncated mutants of Tiam1 to determine the region within Tiam1, which is required for the interaction with ephrin-B1 or EphA2 (Figure 1B). Among the truncated mutants of Tiam1, N-terminal-deleted Tiam1 (C1199) tightly bound to ephrin-B1, but Tiam1 encoding 392 amino-terminal amino acids (N392) did not associate with ephrin-B1 (Figure 1C, lanes 1–4). Reciprocally, EphA2 interacted with Tiam1 (N392), but did not associate with Tiam1 (C1199) (Figure 1C, lanes 5–8). These results indicate that ephrin-B1 and EphA2 interact with different regions of Tiam1.

To identify the region of the Tiam1 protein essential for the interaction with ephrin-B1 or EphA2, we performed an *in vitro* glutathione *S*-transferase (GST) fusion protein pull-down assay. *In vitro*-translated Tiam1 was co-precipitated with the GST-tagged cytoplasmic region of ephrin-B1 (ephrin-B1$^{264-346}$) or EphA2 (EphA2$^{563-977}$) but not by the control GST alone (Figure 2, top). The cytoplasmic region of ephrin-B1 did not bind to Tiam1 (N392). As shown in Figure 2 (bottom), ephrin-B1 clearly associated with the PHnTSS region of Tiam1, which is also included in C1199 and N1041. Therefore, we concluded that the cytoplasmic region of ephrin-B1 binds to Tiam1 via its PHnTSS region. The PHnTSS region contains amino-terminal PH domain, which is known to involve in membrane targeting of Tiam1 protein, and TSS domain, which is conserved among Tiam1, STEF and SIF proteins (Matsuo *et al*, 2002). On the other hand, the GST-tagged cytoplasmic region of EphA2 did not associate with the PHnTSS region of Tiam1, but instead associated with Tiam1 constructs harboring the amino-terminal region of Tiam1 (N392). We assume that EphA2 binds to Tiam1 via its amino-terminal region (Tiam1$^{1-392}$). Although the association of Tiam1 with ephrin-B1 was detected without activation of ephrin-B1 by the extracellular domain (ECD) of EphB2, we found that the GST-tagged PHnTSS domain of Tiam1 expressed in 293T cells was co-precipitated with ephrin-B1 more effectively after the incubation with EphB2-Fc (Supplementary information 3A).

Finally, we examined the *in vivo* status of Tiam1 with ephrin-B1/EphA2 in the E14 mouse brain, where Tiam1 and ephrin-B1 are highly expressed. Tiam1 was co-precipitated with ephrin-B1 from an extract of E14 mouse whole brain by the specific antibody, but not by normal goat serum (Figure 3A). Although EphA2 in the whole brain of E14 mouse is expressed at a low level, endogenously expressed Tiam1 protein was co-immunoprecipitated with EphA2 but not with the control mouse IgG1 (Figure 3B). The interaction of ephrin-B1 and EphA2 with Tiam1 in the mouse brain was further confirmed by experiments using the antibodies in reverse order. Ephrin-B1 and EphA2 were co-precipitated with Tiam1 by the specific antibodies, but not by normal rabbit serum (Figure 3C and D). The size of endogenous ephrin-B1 protein in the mouse brain was slightly larger than transiently expressed ephrin-B1 in COS1 cells.

Tiam1 is translocated after stimulation with the extracellular domain of EphB2 or ephrin-A1

Next, we examined the cellular localization of Tiam1, ephrin-B1 and EphA2. Ephrin-B reverse signaling is known to induce the formation of large membrane patches containing several proteins after stimulation with preclustered EphB2-Fc (Cowan and Henkemeyer, 2002; Palmer *et al*, 2002). In SK-N-MC cells, intense staining of endogenous ephrin-B1 protein is observed in the cell membrane at the contact of cell-to-cell adhesion (Figure 4A, column c, top). Concomitantly with the stimulation of EphB2-Fc, patches containing ephrin-B1 were formed mostly in the cell membrane (Figure 4A, column a, top panel). As expected, the colocalization of ephrin-B1 in patches containing EphB2-Fc was also confirmed in SK-N-MC cells (Supplementary information 2, column a). Tiam1 protein is homogenously expressed in the cytoplasm before

Figure 1 Tiam1 forms a complex with ephrin-B1 and EphA2 receptor. (**A**) COS1 cells were transiently transfected with a plasmid encoding wild-type Tiam1 together with that encoding ephrin-B1 (lanes 1, 2, 5, 6) or EphA2 (lanes 3, 4, 7, 8). Cells were lysed and immunoprecipitated (IP) with anti-ephrin-B1 (goat polyclonal, lane 1), normal goat serum (NGS, lane 2), anti-EphA2 (lane 3), mouse IgG1 (lane 4), anti-Tiam1 (lanes 5, 7) or normal rabbit serum (NRS, lanes 6, 8). The precipitates were subjected to immunoblotting (IB) with the indicated antibodies. The same membranes were reblotted with the antibodies indicated (bottom panels). The expression of Tiam1, ephrin-B1 and EphA2 in the cell lysate was confirmed by immunoblotting. When wild-type ephrin-B1 is overexpressed in COS1 cells, at least two major bands were observed by anti-ephrin-B1 goat polyclonal antibody. Ig, immunoglobulin. The prominent band of 80 kDa in lane 3 is an unknown protein, which associates with EphA2 and may have a related structure with Tiam1. (**B**) Schematic representation of a wild-type and the truncated Tiam1 cDNA constructs used in this study. Proteins are depicted to scale; M, myristoylation signal; PHn and PHc, NH2- and COOH-terminal pleckstrin homology domains; TSS, otherwise known as coiled-coil region and an additional adjacent region (CC-Ex); PDZ, PSD-95/DlgA/ZO-1 domain; DH, Dbl homology domain. (**C**) COS1 cells were transiently transfected with the plasmids as indicated in the above lanes. The cell lysates were immunoprecipitated with anti-ephrin-B1 C18 (lanes 1, 3), EphA2 (lanes 5, 7), normal rabbit serum (lanes 2, 4) or mouse IgG1 (lanes 6, 8) and immunoblotted with anti-myc antibody. The same membranes were reblotted with anti-ephrin-B1 (goat) or anti-EphA2 as indicated. The expression of myc-tagged Tiam1 constructs in these cell lysates (total lysate) was confirmed by immunoblotting. The additional band at 110 kDa in lane 1 may be an artificially produced fragment of overexpressed Tiam1 construct.

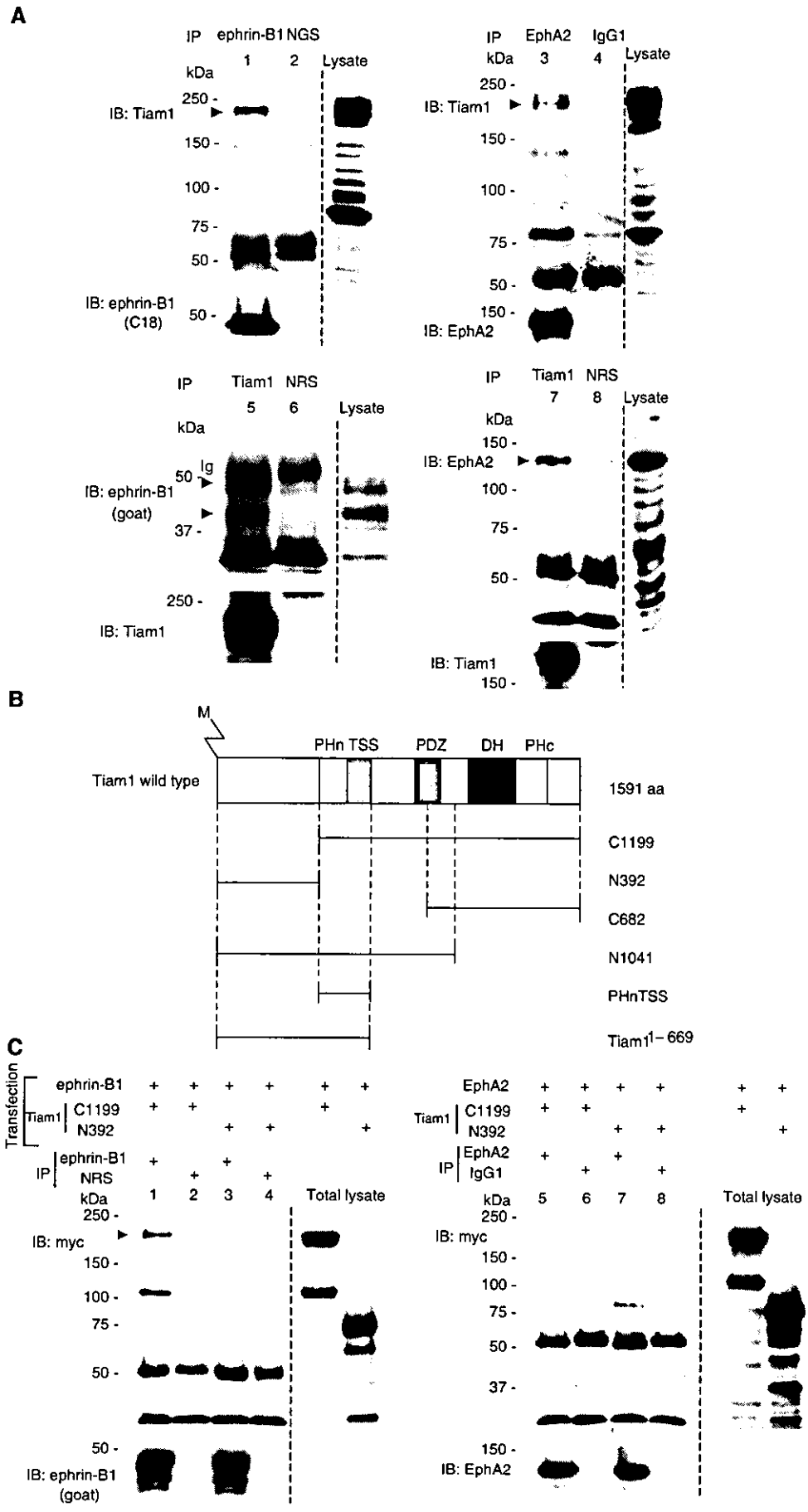

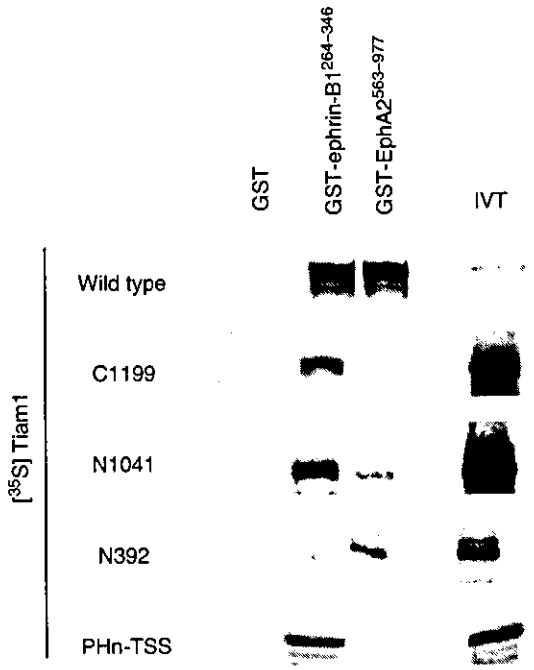

Figure 2 Tiam1 binds to ephrin-B1 and EphA2 *in vitro*: [^{35}S]methionine -labeled wild type or truncated mutants of Tiam1 (C1199, N1041, N392, PHnTSS) translated products were incubated with glutathione-agarose-conjugated GST, GST-ephrin-B1$^{264-346}$ and GST-EphA2$^{563-977}$, respectively. IVT, the input of *in vitro* translation reaction before the beads binding.

stimulation with EphB2-Fc (Figure 4A, column c, middle). However, at least a part of Tiam1 was clearly found to colocalize to the patches after exposure to preclustered EphB2-Fc (Figure 4A, column a, middle and bottom). Although there were a few spotty stains of both ephrin-B1 and Tiam1 in the cells without stimulation of EphB2-Fc, they never colocalized as shown in the merged panel (Figure 4A, column c). In order to exclude the possibility that the second antibodies used directly recognize the clustered Fc fusion proteins, we have shown that there is almost no staining of Tiam1 protein by staining with the secondary antibody without prior incubation with the primary anti-Tiam1 antibody (Figure 4A, column b). We also confirmed that the preincubation of anti-Tiam1 antibody with the blocking peptide (Tiam1 C16) or the bacterially produced GST fusion protein of Tiam1$^{1430-1591}$ containing its C-terminal region abolished Tiam1 staining (data not shown). In the primary cortical neurons from E14 mouse embryos, ephrin-B1 is highly expressed on the cell membrane and neurites, and Tiam1 protein is distributed in the cytoplasm of the cell body and neurites (Figure 4B, columns c and d). Tiam1 and ephrin-B1 were also copatched in E14 cortical neurons 1 h after stimulation with clustered EphB2-Fc (Figure 4B, columns a and b). We observe many patches containing Tiam1 and ephrin-B1 on the elongated neurites and the periphery of cell bodies of these neurons, while there was no such patchy localization of Tiam1 in the neurons without stimulation with EphB2-Fc. In Supplementary information 2, we show the precise colocalization of ephrin-B1 with EphB2-Fc patches, and that in the control there was no crossreaction of the rhodamine-labeled secondary antibody to clustered Fc fusion protein in primary cortical neurons (columns b and c, respectively).

NB1 neuroblastoma cells express EphA2 and Tiam1 endogenously as described later. Before stimulation of NB1 cells with ephrin-A1-Fc, there was no patchy localization of EphA2 detected by immunostaining. Intense staining of EphA2 was located on the cell membrane, especially at the sites of cell-to-cell contact (Figure 4C, column c, top). In the same manner as is the case with cortical neurons, Tiam1, initially distributed homogenously in the cytoplasm (Figure 4C, column c, middle), was partly translocated to patches containing EphA2 after stimulation with soluble ephrin-A1 (Figure 4C, column a, middle and bottom). The patches containing EphA2 localized not only on the cell membrane but also in the cytoplasm, which may be a consequence of the internalization of EphA2 from the cell membrane after stimulation of its ligand. Such internalization of ligand-stimulated EphA2, and more recently ephrin-B1, has been reported (Walker-Daniels *et al*., 2002; Zimmer *et al*., 2003). There was no crossreaction of the secondary antibody to the clustered ephrin-A1-Fc protein (Figure 4C, column b). These results together demonstrate the colocalization of Tiam1 with ephrin-B1 and EphA2, and the distribution of Tiam1 is at least partly translocated after stimulation of ephrin-B1 and EphA2.

Tiam1 is involved in Rac1 activation induced by Eph/ephrin signaling

To analyze whether Eph/ephrin signaling mediates Tiam1 activation, we examined the modification of Tiam1-induced Rac1 activation by the affinity precipitation of GTP-bound Rac1 with the GST-tagged p21-binding domain of PAK1 (GST-PBD). Rac1 was slightly activated by the overexpression of wild-type Tiam1 (Figure 5A, compare lanes 1 and 2). Although Rac1 was also slightly activated after stimulation with EphB2-Fc in ephrin-B1-expressing cells (Figure 5A, lane 3), the amount of GTP-bound Rac1 was markedly increased in response to the stimulation by EphB2-Fc when both Tiam1 and ephrin-B1 are expressed (Figure 5A, compare lanes 4 and 5). Because the PHnTSS region of Tiam1 works as a dominant-negative mutant of Tiam1 (Stam *et al*, 1997), we next examined whether PHnTSS of Tiam1 blocks the Rac1 activity induced by the activation of ephrin-B1. The activation of Rac1 induced by the stimulation of EphB2-Fc was completely abolished by the coexpression of PHnTSS of Tiam1, but not by the coexpression of Tiam1 (N392) (Figure 5A, lanes 8 and 9). The coexpression of EphA2 and Tiam1 did not induce Rac1 activation significantly without stimulation of ephrin-A1-Fc (Figure 5A, lane 10). The overexpression of EphA2 alone is not effective in activating Rac1 even though the cells were stimulated by ephrin-A1 (Figure 5A, lane 15). The stimulation of ephrin-A1-Fc activated Rac1 in cells expressing EphA2 and Tiam1, which was blocked by the coexpression of Tiam1$^{1-669}$ (Figure 5A, compare lanes 11 and 12). The coexpression of PHnTSS partly inhibited the ephrin-A1-Fc-induced Rac1 activation, and Tiam1$^{1-392}$ blocked the Rac1 activation very effectively but not completely (Figure 5A, lanes 13 and 14).

We next examined the phosphorylation of Tiam1 by the activation of ephrin-B1 or EphA2. When ephrin-B1-expressing cells were cocultured with cells expressing kinase-inactivated EphB2 (EphB2K661M), ephrin-B1 was highly phosphorylated on tyrosine residues, but not when cocultured with control mock-transfected cells as we have described before (Figure 5B, lanes 1 and 2, bottom) (Tanaka *et al*, 2003). Similarly, the tyrosine phosphorylation of EphA2 was in-

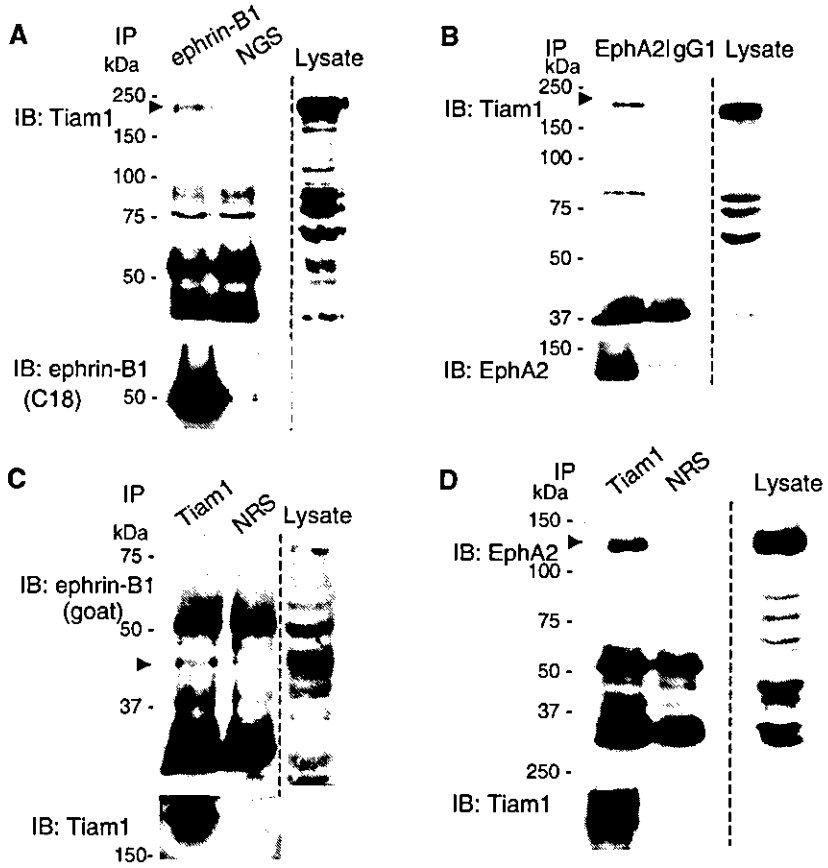

Figure 3 Tiam1 physiologically interacts with ephrin-B1 and EphA2 in the brain of an E14 mouse embryo. Whole brains from E14 mice embryos were lysed and immunoprecipitated (IP) with anti-ephrin-B1 (goat), anti-EphA2, anti-Tiam1, normal goat serum (NGS), normal rabbit serum (NRS) or mouse IgG1 respectively as indicated in the above lanes. The precipitates were subjected to immunoblotting (IB) with the indicated antibodies. Co-precipitated Tiam1, ephrin-B1 and EphA2 are indicated by arrowheads. In (C), the upper band of ephrin-B1 was overlapped with the band of immunoglobulin. The membranes were reblotted with antibodies indicated (bottom panels).

creased when EphA2-expressing cells were cocultured with cells expressing ephrin-A1 (Figure 5B, lanes 5 and 6, bottom). The activation of ephrin-B1 by overlaying the EphB2-expressing cells leads to weak phosphorylation of Tiam1 as detected by labeling cells with orthophosphate (Figure 5B, lanes 1 and 2). Tiam1 is also phosphorylated upon stimulation of EphA2 by coculturing with cells expressing ephrin-A1 (Figure 5B, lanes 3 and 4). Moreover, Tiam1 is phosphorylated on tyrosine residues by the stimulation of EphA2-mediated signaling, as detected by immunoblotting with anti-phosphotyrosine antibody (Figure 5B, lanes 5 and 6). On the other hand, we did not clearly detect phosphorylation of Tiam1 in response to activation of ephrin-B1 on either tyrosine residues (examined by the same method as above) or on serine/threonine residues by immunoblotting with the antibodies described in Supplementary information 1 (data not shown).

Neurite outgrowth by ephrin-B1–Tiam1 and EphA2–Tiam1 interaction

We first confirmed that the dissociated primary cultured cells of E14 cortical neurons still maintain the expression of Tiam1, ephrin-B1, EphB2 and EphA4 *in vitro*, although the expression levels of these proteins were higher in the cortical tissue compared to dissociated cortical cells (Figure 6E). When E14 cortical neurons were seeded on preclustered EphB2-Fc-coated plates, ephrin-B1 is phosphorylated on tyrosine residues at 30 min and 4 h after plating (Figure 6E, bottom). Around 31% of the cells seeded on EphB2-Fc-coated plates show neurites longer than one cell body in length (Figure 6A, Table I), which is statistically different from the numbers when plated on the clustered Fc only or on the albumin (Figure 6B and C). The effect of ephrin-A1-Fc on neurite outgrowth of E14 mouse cortical neurons was weaker than the stimulation of EphB2-Fc (Figure 6D, Table I). In particular, the number of cells bearing longer neurites (longer than three cell bodies in length) was much smaller when cells were seeded on ephrin-A1-Fc-coated plates than on EphB2-Fc-coated plates (Table I). EphA2 expression in the cortex of E14-16 was monitored in brain lysates, because we suspect that the weak expression in this area and the developmental stage may be one of the reasons for the less dramatic effect on neurite outgrowth. Actually, the expression of EphA2 was barely detectable in the cortex region of this stage (Figure 6E), while it was detectable in the whole brain lysate (Figure 3). We did not observe any elongated neurites on ephrin-B1-Fc-coated plates (data not shown).

In the neuroblastoma cell line NB1, a considerable expression of Tiam1 and EphA2 was detected (Figure 7D). We also confirmed that NB1 cells do not express detectable level of EphA4 (Figure 7D). We used this NB1 system in the following experiments for evaluation of EphA2 forward signaling. The

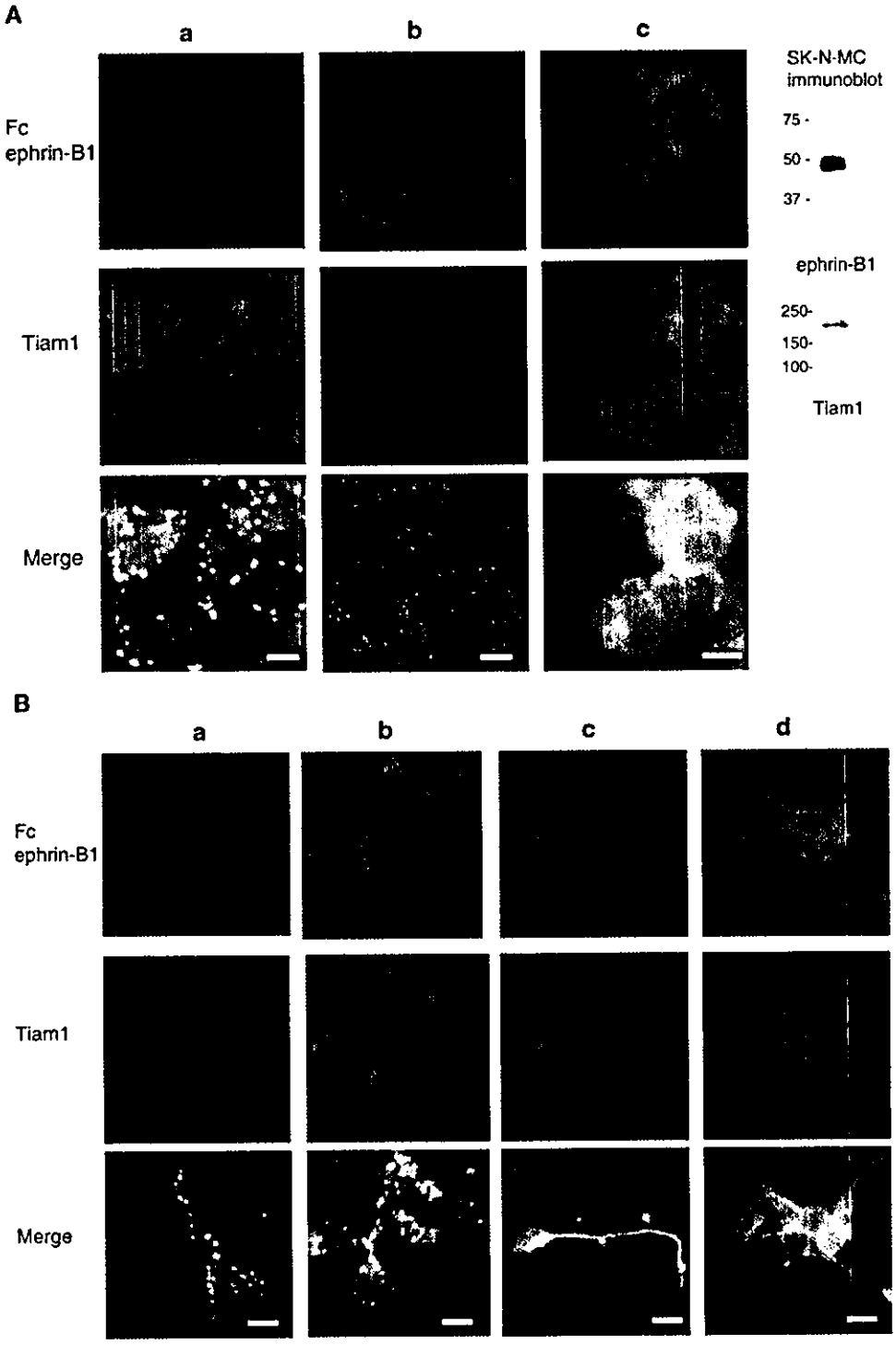

Figure 4 Tiam1 is recruited to patches induced by EphB2-Fc- or ephrin-A1-Fc stimulation. (**A**) SK-N-MC cells expressing ephrin-B1 were stimulated with 4 μg/ml of clustered EphB2-Fc (columns a, b) or left untreated (column c). After 10 min of stimulation, the cells were washed and incubated in a medium without EphB2-Fc for 1 h prior to fixation. The cells were immunostained with anti-Fc (green) and anti-Tiam1 (red) antibodies (column a). In column b, incubation with primary anti-Tiam1 antibody was omitted prior to incubation with the rhodamine-labeled secondary antibody. Column c shows the signals with anti-ephrin-B1 staining (green) and anti-Tiam1 staining (red). Expressions of Tiam1 and ephrin-B1 in SK-N-MC cells are shown by immunoblot. (**B**) (Columns a, b) E14 mouse cortical neurons were cultured for 20 h on poly-L-lysine-coated slides, and then stimulated with EphB2-Fc for 1 h as described above. The cells were fixed and immunostained with anti-Fc (green) and anti-Tiam1 (red) antibodies. (Columns c, d) Localization of ephrin-B1 (green) and Tiam1 protein (red) without stimulation of EphB2-Fc is shown. (**C**) (Columns a, b) NB1 neuroblastoma cells were stimulated with 4 μg/ml of clustered ephrin-A1-Fc as described in (**A**). The cells were immunostained with anti-Fc (green) and anti-Tiam1 (red) antibodies. In column b, incubation with primary anti-Tiam1 antibody was omitted prior to incubation with the rhodamine-labeled secondary antibody. (Column c) Localization of EphA2 (green) or Tiam1 protein (red) without stimulation of ephrin-A1-Fc is shown. Scale bar, 10 μm.

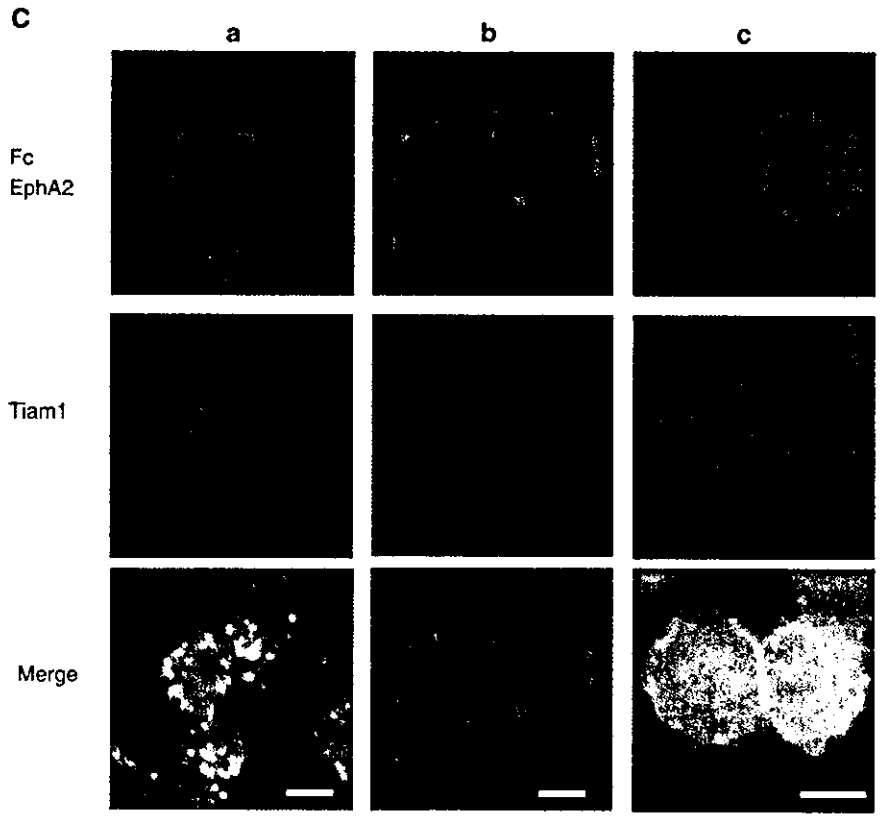

Figure 4 (Continued)

tyrosine phosphorylation of EphA2 was clearly demonstrated at 30 min and 4 h after plating on ephrin-A1-Fc-coated dish (Figure 7D, bottom). The decreased expression level of EphA2 after stimulation is considered to be a result of negative regulation of activated EphA2 by Cbl-mediated ubiquitination (Wang *et al*, 2002). When NB1 cells were plated on a surface coated with preclustered ephrin-A1-Fc, many cells exhibited long thin neurites after 16 h of incubation (Figure 7B), whereas few cells bearing such neurites were observed in cells plated on the control Fc-coated plates (Figure 7A). The elongated neurites were not observed on preclustered EphA2-Fc-coated plate, either, as shown in Figure 7C.

To confirm that the outgrowth of neurites observed above depends on the interaction of EphB2 or ephrin-A1 with its cognate ligand or receptor, we did several experiments interfering with this pathway by a soluble ligand or receptor and a dominant-negative or defective competitor in the following experiments. When the cells were plated on Fc fusion protein-coated surface as above with an excess volume of the soluble ephrin-B1-Fc or EphA2-Fc in the medium, the neurite outgrowth of E14 cortical neurons plated on the EphB2-Fc surface and neurite outgrowth of NB1 cells plated on the ephrin-A1-Fc surface were blocked, respectively. However, the addition of soluble ephrin-B1 or EphA2 in the medium had no effect on the nonspecific neurite outgrowth of E14 cortical neurons and NB1 cells induced by plating cells on a poly-L-lysine-coated surface (data not shown). Furthermore, the forced expression of an ephrin-B1 mutant lacking its cytoplasmic region (ephrin-$B1^{1-265}$) in E14 mouse cortical neurons lessened the effect both in numbers and length of neurites, while the expression of control EGFP did not affect the neurite outgrowth (Figure 8, compare A and B). Likewise, the expression of mutants of EphA2 lacking its cytoplasmic region ($EphA2^{1-540}$) in neuroblastoma cells reduced the number of these cells bearing neurites on an ephrin-A1-coated surface (Figure 8, compare E and F).

Finally, we examined whether dominant-negative mutants of Tiam1 inhibit the neurite outgrowth induced by the ephrin-B1- or EphA2-mediated signaling. E14 cortical neurons on the EphB2-Fc surface were transiently transfected with the PHnTSS region of Tiam1 tagged with EGFP. On the other hand, we used $Tiam1^{1-669}$ to test whether it could block the neurite outgrowth induced by EphA2-mediated signaling, because it effectively blocked the Rac1 activation induced by the activation of EphA2 (Figure 5A). As shown in Figure 8C, the neurite outgrowth of cortical neurons on the EphB2-Fc surface was significantly inhibited by the expression of PHnTSS protein. Similarly, NB1 cells expressing $Tiam1^{1-669}$ did not show apparent neurites on the ephrin-A1-Fc-coated surface (Figure 8G). On the other hand, the expression of these Tiam1 fragments did not effectively inhibit the nonspecific neurite outgrowth of cortical neurons and NB1 cells induced by plating the cells on poly-L-lysine-coated plates (data not shown). Moreover, the inhibitory effect of PHnTSS protein on the neurite outgrowth of NB1 cells on the ephrin-A1-Fc-coated surface was modest, and we did not observe any inhibition of neurite outgrowth by $Tiam1^{1-392}$ in cortical neurons on the EphB2-Fc-coated surface (data not shown). Taken together, these results (Figure 8D and H)

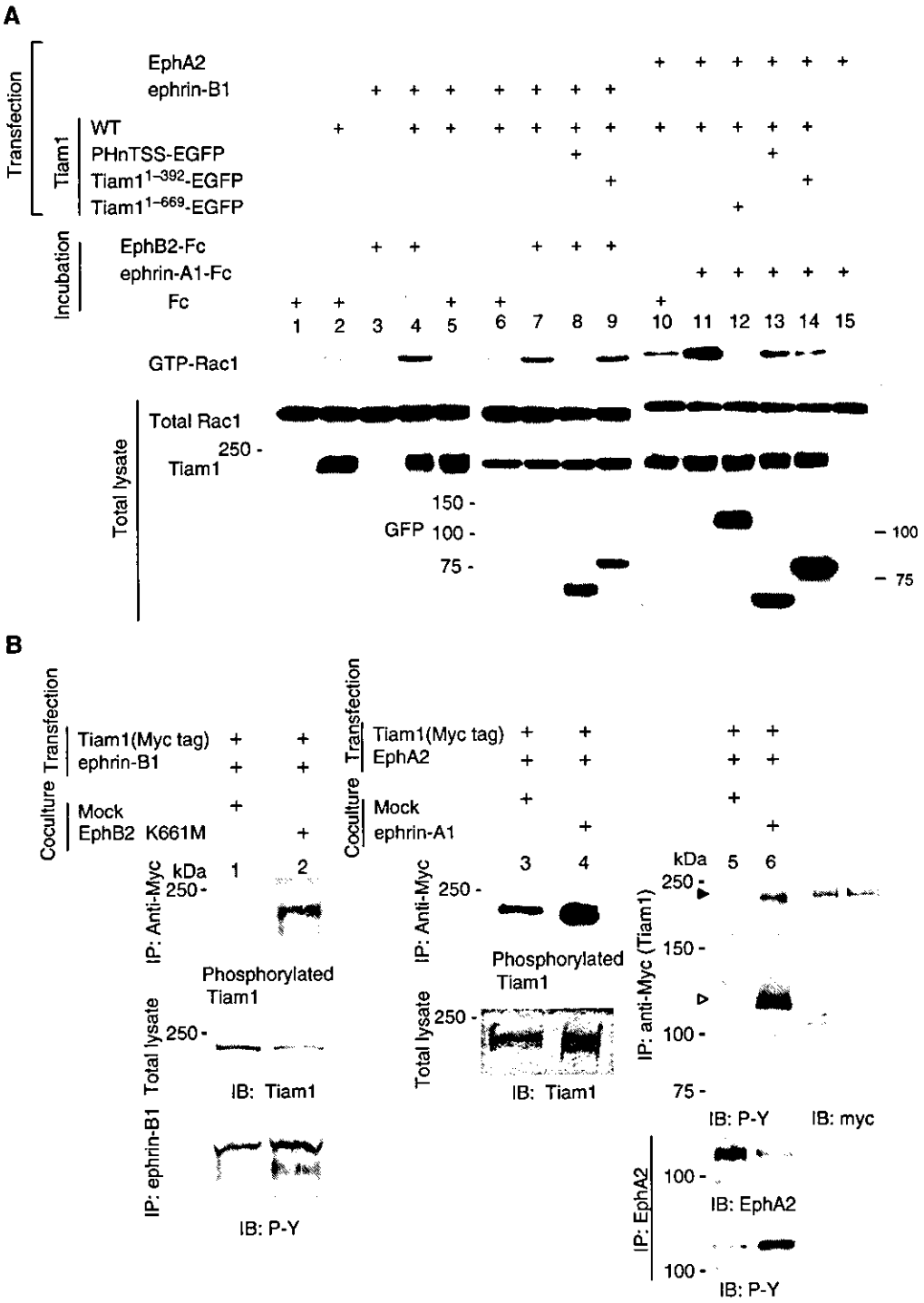

Figure 5 Tiam1 mediates Eph/ephrin-mediated signaling cascades leading to Rac1 activation. (**A**) COS1 cells were transiently transfected with 2 μg of a plasmid encoding wild-type Rac1, together with plasmids indicated in the above lanes. Mock plasmid was used to adjust the amount of DNA to total 10 μg for each transfection. The transfected cells were incubated in media containing clustered EphB2-Fc, ephrin-A1-Fc or control Fc each at a concentration of 5 μg/ml as indicated above the lanes for 15 min before harvesting the cell lysates for affinity precipitation with immobilized GST-PBD. Precipitated GTP-bound Rac1 was detected by immunoblotting with anti-Rac1 antibody. Expression of total Rac1 and Tiam1 is shown at the bottom. (**B**) Phosphorylation of Tiam1 induced by the activation of ephrin-B1 or EphA2 *in vivo*. 293T cells transfected with the plasmids indicated at the top were cocultured with the 293T cells (lane 1), the 293T cells stably expressing EphB2 K661M (lane 2), the NIH3T3 cells (lanes 3, 5) or the NIH3T3 cells stably expressing ephrin-A1 (lanes 4, 6). Lanes 1–4: The coculture was performed in media containing $^{32}P_i$ for 4 h, and then the cells were lysed for immunoprecipitation with anti-myc, separated by SDS–PAGE and visualized by autoradiography. Lanes 1, 2 bottom: The lysates for immunoprecipitation were prepared from the cells as described above except for the labeling with $^{32}P_i$. Lanes 5, 6: The coculture was performed for 30 min before cell lysates were immunoprecipitated with anti-myc and immunoblotted with anti-phospho-tyrosine antibody (4G10). The phosphorylation of Tiam1 is indicated by filled triangle. Co-precipitated EphA2 is indicated by open triangle. The same membrane was reblotted with anti-myc antibody (right panel). The phosphorylation of ephrin-B1 and EphA2 on tyrosine residues is shown at the bottom of lanes 1, 2 and lanes 5, 6, respectively.

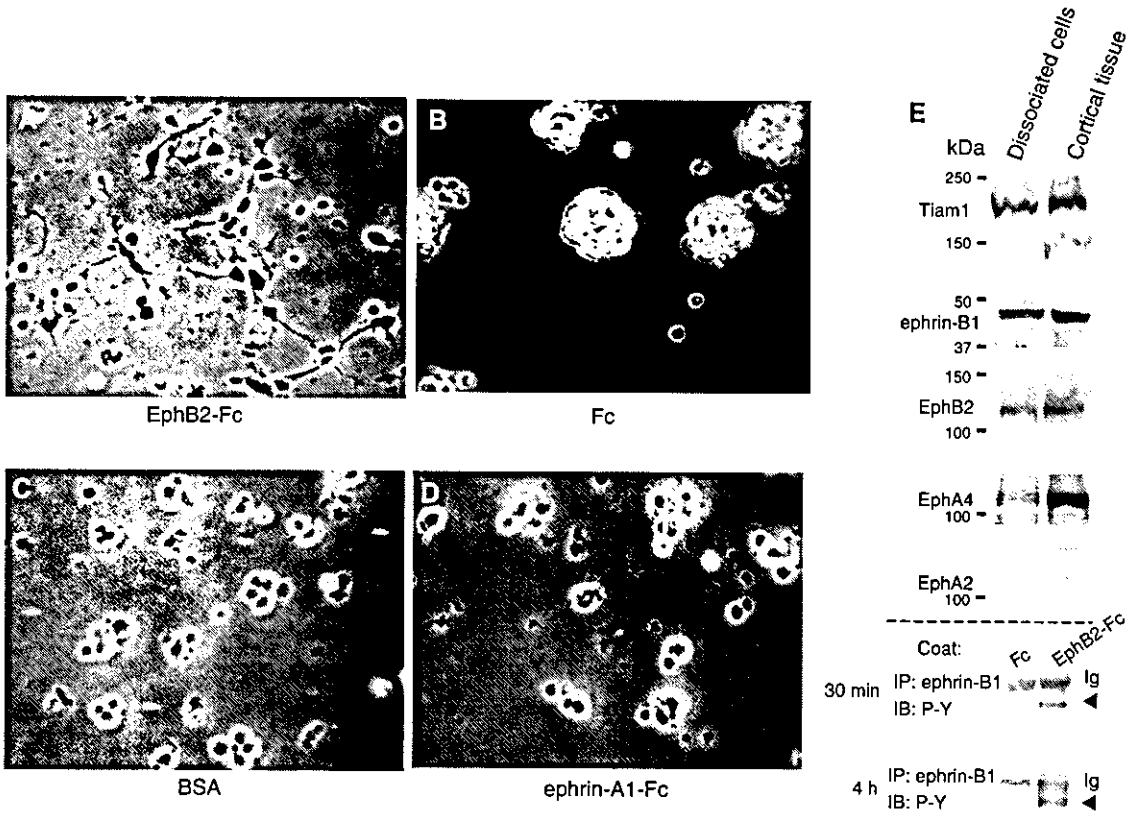

Figure 6 EphB2-Fc induces neurite outgrowth of E14 mouse cortical neurons. Primary cultured cortical neurons from E14 mouse cerebral cortex were seeded on plates coated with EphB2-Fc (**A**), Fc fragment (**B**), bovine serum albumin (BSA) (**C**) or ephrin-A1-Fc (**D**), as described in Materials and methods (Neurite elongation assay). Representative pictures are shown after incubation for 20 h (A–D). (**E**) Expression of Tiam1, ephrin-B1 and various Eph receptors in dissociated primary cultured cells after 20 h incubation on poly-L-lysine-coated dishes, or in the cortical tissues was monitored by immunoblotting. (E, bottom) E14 primary precursors plated on an EphB2-Fc-coated dish were lysed for the indicated period, and immunoprecipitated with anti-ephrin-B1. Tyrosine phosphorylation of ephrin-B1 is shown by immunoblotting.

Table I Quantification of the effects of EphB2-Fc and ephrin-A1-Fc on neurite formation

	Three cell bodies/ total counted[a]	One cell body/total counted[a]
E14 primary cortical neuron[b]		
Fc	0/527 (0%)	0/527 (0%)
BSA	0/531 (0%)	31/531 (5.8%)
EphB2-Fc	61/552 (11.1%)	173/552 (31.3%)
ephrin-A1-Fc	10/523 (1.95)	99/523 (18.9%)
NB1 neuroblastoma cell line[c]		
Fc		0/323 (0%)
ephrin-A1-Fc		115/349 (33.0%)
EphA2-Fc		14/304 (4.6%)

[a]The number of cells possessing neuritis three cell bodies or one cell body was counted 20 h after plating the cells.
[b]Total number of cells counted in four independent experiments.
[c]Total number of cells counted in three independent experiments.

indicate that Tiam1 locates downstream of ephrin-B1- or EphA2-mediated signaling and is involved in the neurite outgrowth.

Discussion

Examination of the association between Tiam1 with ephrin-B1 and EphA2 receptor revealed that Tiam1 interacts with ephrin-B1 and EphA2. Interaction of Tiam1 with EphA2 was not apparently modified by the phosphorylation status of EphA2, because EphA2 with a mutation in its kinase domain and an abolished catalytic activity also associated with Tiam1 as well as wild-type EphA2 (data not shown). However, we cannot completely exclude the possibility that the association of Tiam1 with ephrin-B1 is increased by the stimulation of EphB2-Fc (Supplementary information 3A). The observations that staining of Tiam1 in the cytoplasm did not appear to diminish in the stimulated cells (Figure 4) reveal that only a part of Tiam1 protein translocated to the patches colocalizing with ephrin-B1 or EphA2. Therefore, the localized activation of Tiam1 and Rac1 should be monitored spatially and temporally in these cells in order to evaluate the significance of the translocation of Tiam1. In primary cultured cortical neurons, patches containing ephrin-B1 and Tiam1 often locate along the extended neurites. The biological significance of such colocalization along the neurites requires elucidation. Although Tiam1 is clearly phosphorylated on tyrosine residues by EphA2 activation, we detected phosphorylation of Tiam1 in ephrin-B1-activated cells at low level only by the orthophosphate labeling (Figure 5B). Because the phosphorylation of Tiam1 on threonine residues has been detected by the same antibody in response to the stimulation of platelet-derived growth factor, Tiam1 was not phosphorylated at least on the same positions by the activation of ephrin-B1 (Fleming *et al*, 1998). The significance of the

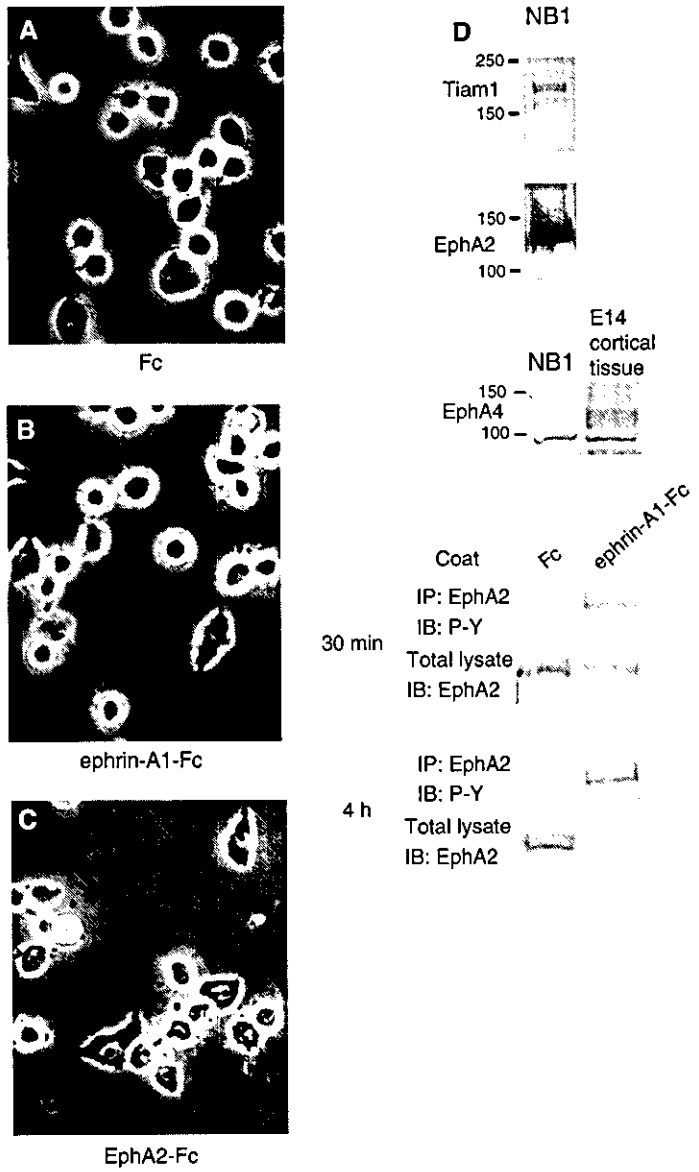

Figure 7 Ephrin-A1-Fc induces neurite outgrowth of NB1 neuroblastoma cells. NB1 neuroblastoma cells were seeded on plates coated with Fc fragment (**A**), ephrin-A1-Fc (**B**) or EphA2-Fc (**C**) as described in Materials and methods. Representative cells are shown after incubation for 20 h (A–C). (**D**) Expression of Tiam1 and Eph receptors in NB1 cells is shown by immunoblotting. (D, bottom) The NB1 cells plated on ephrin-A1-Fc-coated dishes were lysed for the indicated period, and immunoprecipitated with anti-EphA2. Tyrosine phosphorylation of EphA2 is shown by immunoblotting.

phosphorylation of Tiam1 induced by the activation of ephrin-B1 and EphA2 remains to be further studied.

Among proteins reported to be putatively associated with the cytoplasmic regions of Ephs or ephrins, Ephexin, which is a GEF for the rho family GTPases, preferentially interacts with EphA receptors (Shamah *et al*, 2001). Stimulation of ephrin-A regulates growth cone collapse or retraction through Ephexin. Although A-class ephrins are not highly expressed in the developing mouse cortex (Yun *et al*, 2003), it is important to examine the expression of Tiam1 and Ephexin, two exchange factors having opposing effects on the neurites motility, in the cortical region. Furthermore, we also have to consider a homologous protein of Tiam1, STEF, another GEF for Rac1, because STEF is also expressed in the cerebral cortex of developing mice (Matsuo *et al*, 2002; Kawauchi *et al*, 2003). We detected the association of the PHnTSS domain

Figure 8 Expression of dominant-negative mutants of ephrin-B1, EphA2 and Tiam1 affects EphB2-Fc- or ephrin-A1-Fc-induced neurite outgrowth. Primary cultured cortical neurons from E14 mouse embryos (**A–D**), or NB1 cells (**E–H**) were transfected with plasmids encoding either EGFP, EGFP-tagged mutants of ephrin-B1 or EphA2, which lack the cytoplasmic regions (ephrin-B1$^{1-265}$-EGFP, EphA2$^{1-563}$-EGFP), or EGFP-tagged fragments of Tiam1 (PHnTSS-EGFP or Tiam1$^{1-669}$-EGFP). The transfected cells were fixed after 20 h of incubation on slides coated with either EphB2-Fc (A–D) or ephrin-A1-Fc (E–H), and observed through a fluorescence microscope. Representative cells are shown (A–C, E–G). (D, H) Percentage of transfected cells bearing neurites longer than one cell body. Exogenously expressed proteins in these cells were monitored by immunoblotting.

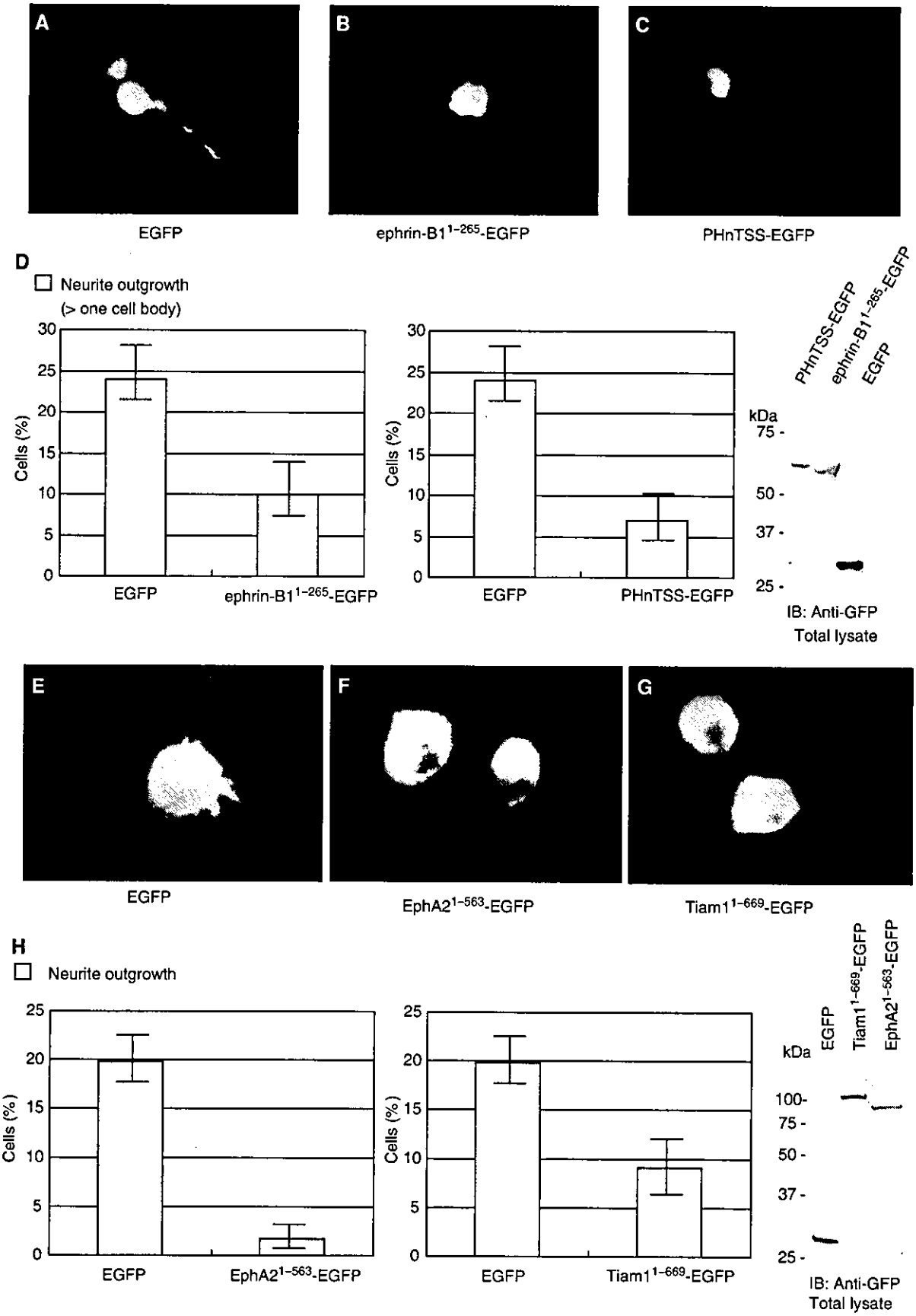

of STEF with ephrin-B1 by immunoprecipitation analysis (Supplementary information 3B). Therefore, the neurite outgrowth may be regulated by exchange factors other than or in addition to Tiam1 in a certain region and stage. In this report, we have used Tiam1 fragments containing the PHnTSS region ($Tiam1^{431-669}$ and $Tiam1^{1-669}$) to block wild-type Tiam1. Because the PHnTSS region of Tiam1 is highly homologous to the PHnTSS domain of STEF, these Tiam1 fragments may also work as dominant-negative mutants for STEF. In addition, we cannot exclude the possibility that Tiam1 fragments containing PHnTSS might antagonize the binding of ephrin-B1 or EphA2 to Tiam1 in addition to acting as a dominant-negative for Tiam1.

The molecular mechanism of the activation of Tiam1 in ephrin-B1- and EphA2-mediated signaling is not clear. Although PHnTSS region is not involved in the association of Tiam1 with EphA2, the expression of PHnTSS inhibited EphA2-induced Rac1 activation mildly, but evidently (Figure 5A). This result may suggest the possibility that EphA2 also activates Tiam1 by a mechanism independent of their association. EphA2 interacts with the p85 subunit of phosphatidylinositol-3-kinase (PI3-kinase) and induces the activation of PI3-kinase (Pandey *et al*, 1994). On the other hand, Tiam1 has been reported to activate by the lipid products of PI3-kinase *in vitro* (Fleming *et al*, 2000). Because PHn (amino-terminal PH domain) is required for the membrane localization and the binding of Tiam1 to the lipid products of PI3-kinase (Stam *et al*, 1997), the overexpression of PHnTSS is considered to block PI3-kinase-dependent Tiam1 activation. Therefore, the inhibitory effect by N392-PHnTSS ($Tiam1^{1-669}$) on the neurite outgrowth of NB1 cells may include a mechanism that may not depend on the association of Tiam1 with EphA2 (Figure 8). However, as shown in Figure 5A, overexpression of N392 alone abolished the Rac1 activation more effectively than PHnTSS. Therefore, the significance of the PI3-kinase for the activation of Tiam1 in EphA2-mediated signaling should be further elucidated.

Concerning the ephrin-B1-mediated reverse signaling on retinal axon growth, both repulsive and attractive guidance has been previously suggested. Birgbauer *et al* (2001) have shown that the ECD of EphB receptors as soluble proteins induced growth cone collapse of ephrin-B-expressing retinal ganglion cells. They also show that axon outgrowth of ephrin-B-expressing dorsal retina explants of E14 mouse was inhibited on the laminin substratum containing EphB-ECD. On the other hand, Mann *et al* (2002) propose an attractive axon guidance that requires the ephrin-B cytoplasmic domain. Retinal axons of *Xenopus* expressing ephrin-Bs prefer to grow on laminin substratum containing EphB receptor stripes *in vitro*. These apparently inconsistent observations may be due to the differences in the experimental procedures, and not to those in the species used between these reports. EphB-Fc protein was used as a dimer in the former (Birgbauer *et al*, 2001) and as a multimer by preclustering with immunoglobulin in the latter (Mann *et al*, 2002); the concentration of laminin substratum used in these reports was also different. In the present study, we followed a procedure similar to that of Mann *et al*, and devised a simplified system for evaluating the outputs of Eph/ephrin-induced signaling. We found that ephrin-B1-expressing cortical neurons markedly extend neurites on surfaces coated with preclustered EphB2-Fc without any other substratum. As to the laminin concentration, the substratum we used contained no laminin, more similar to that used by Mann *et al* (1 μg/ml) than that used by Birgbauer *et al* (10 μg/ml). The lower concentration of laminin seems to prefer the more attractive or progrowth reaction of these systems.

Cell adhesion itself may promote neurite growth, and there are reports concerning adhesive interactions between ephrin-B-expressing axons and the substrate-bound Eph receptor (Holash *et al*, 1997). We also noticed faster attachment of dissociated E14 cortical neurons on EphB2-Fc-coated plates compared to that on Fc-coated plate. We have not directly examined whether Tiam1 mediates this cell-to-substrate adhesion of the cortical neurons, but the adhesion of cortical neurons on the EphB2-Fc surface was accompanied by the phosphorylation of the tyrosine residues of $p130^{Cas}$ and focal adhesion kinase (Supplementary information 4). The primary cultured cortical neurons of E14 mouse embryos adhered to the plates to almost the same degree as a few hours after plating and thereafter, irrespective of whether plates were coated with preclustered-EphB2-Fc, -ephrin-A1-Fc or bovine serum albumin (BSA). Similarly, NB1 cells adhered almost equally to plates precoated with Fc, ephrin-A1-Fc or EphA2-Fc after a few hours of seeding and thereafter. However, we cannot completely exclude the possibility that the differences in neurite outgrowth could depend on differential adhesiveness of the substrates.

Among other members of Eph receptors and ephrins, considerable expression of ephrin-B2 and ephrin-B3 mRNAs is also present in the cortical neurons (Stuckmann *et al*, 2001). Moreover, EphA4 protein is broadly expressed within the cortex of E14 and E16 mouse (Liebl *et al*, 2003; Yun *et al*, 2003). Because the amino-terminal region of Tiam1 ($Tiam1^{1-392}$) also associates with EphA4 leading to the phosphorylation of Tiam1 on tyrosine residues (data not shown), EphA4 receptor may also regulate Rac1 activation by interaction with Tiam1. Further studies are necessary to examine whether Tiam1 also regulates signals mediated by ephrin-B2, ephrin-B3 and EphA4 in the neurons, which may position Tiam1 as a general mediator of Eph/ephrin signals. In NB1 cells, we cannot exclude the possibility that neurite outgrowth of NB1 cells was not exclusively mediated by EphA2.

Our results suggest the importance of Tiam1 and Rac1 as downstream molecules in ephrin-B1- or EphA2-mediated signaling in neurite outgrowth. According to previous information, Eph receptors/ephrins signals, both forward and reverse, have exhibited various, sometimes paradoxical effects on the regulation of neurite extension, that is, retraction and elongation. Our discovery of the involvement of Tiam1 downstream with both the forward and reverse signals of Eph/ephrin system in these neurite responses provides insight that the selection of the GEFs actually working downstream to Ephs/ephrins may determine the fate of neurites.

Materials and methods

Plasmids and antibodies

Plasmids and antibodies used in these series of experiments are described in Supplementary information 1.

Cell culture and transfection

SK-N-MC neuroepithelioma cells and NB1 neuroblastoma cells were cultured in RPMI 1640 supplemented with 10% fetal bovine serum.

The cerebral cortex from E14 DDY mouse embryos were dissected, dissociated and plated on chamber slides as described (Ueki *et al*, 1993), and cultured in DMEM supplemented with D-glucose (4.5 g/l) and 10% fetal bovine serum. For transient expression assays, NB1 cells were transfected with plasmid DNA using Lipofectamine 2000 (GIBCO-BRL), and 293T cells and COS1 cells were transfected with plasmid DNA either by a calcium phosphate co-precipitation method essentially as described previously (Otsuki *et al*, 2001) or using FuGENE6 reagent (Roche). For the transfection of plasmid DNA into E14 primary cortical neurons, a total of 3 μg of plasmid DNA and 4 μl Lipofectamine 2000 reagent were each diluted in 50 μl of OPTI-MEM™ (GIBCO-BRL), and applied to the cells cultured in 400 μl of NEUROBASAL with B27 supplement 3 h after plating. The medium was completely exchanged at 4.5 h after transfection, and cells were maintained in DMEM supplemented with D-glucose (4.5 g/l) and 10% fetal bovine serum. NIH3T3 cells stably expressing ephrin-A1 and 293T cells stably expressing EphB2 were established by transfection of pAlterMax encoding EphA2 or EphB2 as described above. Cells were cultured and selected in DMEM containing puromycin at a concentration of 2 μg/ml (for 293T cells) or G418 (Gibco BRL) at 0.6 mg/ml (for NIH3T3 cells) for 2–3 weeks. Well-isolated colonies were characterized further.

Immunoprecipitation and affinity precipitation

Transfected cells were harvested 48 h after transfection, and cell lysates were prepared with protease inhibitors in TXB buffer (10 mM Tris (pH 7.6), 150 mM NaCl, 5 mM EDTA (pH 8.0), 10% glycerol, 1 mM Na_3VO_4 and 1% Triton X-100). Whole brain tissue from E14 DDY mice was also lysed in TXB buffer with a Dounce homogenizer. The lysates were precleared by incubating them with protein G agarose (Boehringer Mannheim) for 1 h at 4°C. To purify the proteins, 1 μg of monoclonal or affinity-purified polyclonal antibodies was added and incubated with 500 μl of cell lysate for 1 h at 4°C. The antibodies were precipitated with protein G agarose for 2 h at 4°C. Immunoprecipitates were extensively washed with TXB buffer, separated by SDS–polyacrylamide gel electrophoresis (PAGE) and immunoblotted.

Affinity precipitation with GST-PBD was performed as described previously (Otsuki *et al*, 2001). Briefly, 293T cells were lysed in the lysis buffer (20 mM Tris–HCl (pH 7.5), 150 mM NaCl, 20 mM $MgCl_2$, 1 mM Na_3VO_4, 5% Triton X-100, 5 μg/ml aprotinin and 1 mM PMSF), and incubated with GST-PBD on sepharose for 1 h at 4°C. The precipitants were washed four times in the same buffer, and endogenous Rac1 protein was detected by immunoblotting.

In vivo phosphate labeling

Plasmids encoding Myc-tagged Tiam1 with ephrin-B1 or EphA2 were transfected into 293T cells in a 35 mm diameter dish. At 48 h after transfection, the transfected cells were cocultured with cells stably expressing EphB2 K661M or ephrin-A1. Transfected cells were preincubated in phosphate-free medium (GIBCO-BRL) for 15 h, and then coculture was performed in 0.5 ml of phosphate-free MEM containing 0.09 mCi of $^{32}P_i$ (NEN) for a further 4 h. The cells were lysed in the lysis buffer (20 mM Tris–HCl (pH 7.5), 150 mM NaCl, 20 mM $MgCl_2$, 1 mM Na_3VO_4, 0.5% Triton X-100, 5 μg/ml aprotinin and 1 mM PMSF). Myc-tagged Tiam1 was purified by immunoprecipitation using an anti-Myc antibody and separated on SDS–PAGE. $^{32}P_i$-labeled Tiam1 was visualized with a Bio Imaging Analyzer (BAS1000, Fuji) (lanes 1 and 2).

Cell staining

To examine the localization of Tiam1 after activation of ephrin-B1 or EphA2, cortical neurons from E14 DDY mice or NB1 cells were seeded on chamber slides. Cells were incubated with 4 μg/ml of clustered EphB2-Fc or ephrin-A1-Fc for 10 min, and then the medium was removed and further incubated in DMEM containing 10% FBS for the indicated period. Cells were fixed for 5 min at room temperature with 4% paraformaldehyde (PFA) in PBS and permeabilized for 5 min with 0.2% Triton X-100. The cells were preincubated in 2% BSA with 5% normal serum for 1 h, and incubated with the FITC-conjugated anti-Fc fragment of IgG antibody for 1 h at room temperature. In some experiments, cells were further stained for Tiam1 protein by sequential incubation with anti-Tiam1 (C-16) antibody and rhodamine-conjugated secondary antibody for 1 h for each. Photos were taken with Radiance 2100 confocal microscope (BioRad).

Neurite elongation assay

Plates and glass chamber slides were coated with Fc fusion proteins, by being filled with 5 μg/ml of Fc fusion proteins or the control Fc fragment plus 50 μg/ml of goat anti-IgG Fc (ICN) in sterile PBS(−) with gentle rocking for 1–2 h at room temperature before the protein solution was aspirated. Plates and chamber slides were washed three times with sterile PBS, and then incubated in PBS containing 2% (w/v) BSA for 30 min at room temperature to block the remaining protein-binding sites. Cortical neurons from the E14 mouse embryos were plated on the coated surface, and then fixed in 4% PFA in PBS after 20 h of incubation. In some experiments, cortical neurons were transfected with EGFP-tagged plasmids indicated as described above 3 h after plating on chamber slides, and then fixed after 20 h of transfection. For the statistical calculations, cells bearing neurites longer than one or three cell bodies in length were considered as cells with neurite outgrowth. In counting, only cells positive for EGFP were included in the analysis.

Supplementary data

Supplementary data are available at *The EMBO Journal* Online.

Acknowledgements

We thank Drs T Pawson (Mount Sinai Hospital), R Klein (European Molecular Biology Laboratory), N Kawazoe and N Nakaya (Laboratory of Biological Chemistry, School of Pharmaceutical Sciences, Showa University), M Hoshino (Department of Pathology and Tumor Biology, Graduate School of Medicine, Kyoto University) and Y Dobashi (Yamanashi University) for providing plasmids and cells used in this study. We thank Dr Ueki (First Department of Anatomy, Hamamatsu University School of Medicine) for assisting with the primary neuron culture technique from mouse embryos, and Associate Prof. Yamamoto (Laboratory of Cell Imaging, Photon Medical Research Center, Hamamatsu University School of Medicine) for assisting with the operation of the fluorescent microscope. We thank Prof. Nakahara (Department of Psychology, Hamamatsu University School of Medicine) for careful reading of this paper. We thank Prof. Sato (First Department of Anatomy, Hamamatsu University School of Medicine), Prof. Tsutsui and Dr Kosugi (Second Department of Pathology, Hamamatsu University School of Medicine) for useful discussion. This work was supported by the Smoking Research Foundation, Grants-in-Aid for Cancer Research from the Ministry of Health and Welfare of Japan, a Grant-in Aid-for Scientific Research (B, 10470056) on Priority areas (C-2, 12218215; C-2, 13216044), and COE (Medical Photonics, Hamamatsu University School of Medicine) from the Ministry of Education, Culture, Sports Technology and Science of Japan, and a Grant-in Aid-for Scientific Research (C2, 14570183) from the Japan Society for the Promotion of Science.

References

Birgbauer E, Oster SF, Severin CG, Sretavan DW (2001) Retinal axon growth cones respond to EphB extracellular domains as inhibitory axon guidance cues. *Development* **128**: 3041–3048

Cheng HJ, Nakamoto M, Bergemann AD, Flanagan JG (1995) Complementary gradients in expression and binding of ELF-1 and Mek4 in development of the topographic retinotectal projection map. *Cell* **82**: 371–381

Cowan CA, Henkemeyer M (2002) Ephrins in reverse, park and drive. *Trends Cell Biol* **12**: 339–346

Fleming IN, Elliott CM, Exton JH (1998) Phospholipase C-γ, protein kinase C and Ca^{2+}/calmodulin-dependent protein kinase II are involved in platelet-derived grpwth factor-induced phosphorylation of Tiam1. *FEBS Lett* **429**: 229–233

Fleming IN, Gray A, Downes CP (2000) Regulation of the Rac1-specific exchange factor Tiam1 involves both phosphoinositide